

Supporting Information

The Dynamic Ligand Field of a Molecular Qubit: Decoherence Through Spin–Phonon Coupling

Ruben Mirzoyan and Ryan G. Hadt *

*Division of Chemistry and Chemical Engineering, Arthur Amos Noyes Laboratory of Chemical Physics,
California Institute of Technology, Pasadena, California, 91125, United States*

Corresponding Author: rghadt@caltech.edu

Table of Contents

<i>A. Computational Methods</i>	3
<i>B. Tables.....</i>	4
<i>C. Figures</i>	40
<i>D. DFT Structures and Input Coordinates</i>	63
<i>E. Representative ORCA Input Files</i>	82
<i>References</i>	85

A. Computational Methods

All DFT calculations were carried out using ORCA¹, version 4.0.1.2 on the High Performance Computing Cluster at Caltech. For the special case of vanadyl phthalocyanine (VOPc) frequency calculations, the version used was 4.1.2 to resolve a glitch involving jobs running on multiple nodes. Representative input parameters for optimization, frequency and single point calculations are provided in the “Representative Orca Input Files” section of this document. For Cu(II) complexes, the Hartree-Fock exchange in the B3LYP functional²⁻⁵ was modified to 38%, except in the cases of thiolate and selenate ligands for which it was left at 20%. For all V(IV) complexes, the Hartree-Fock exchange was modified to 60%. As shown previously,⁶ for values of Hartree-Fock exchange must be determined independently for complexes that exhibit strongly variable covalencies of their respective ligand–metal bonds. All calculations were carried out using the def2-TZVP basis set⁷ with auxiliary basis set def2/J on all atoms.⁸ DFT grid 7 and tight SCF convergence criteria corresponding to a convergence tolerance of 10⁻⁸ Hartrees were used for all calculations.

The calculated normal modes q_k are presented in ORCA as cartesian displacements weighted by the diagonal matrix $M(i, i) = \frac{1}{\sqrt{m[i]}}$, where $m[i]$ is the mass of the displaced atom.

$$Q = \sum_i c_i q_i$$

$$q_i = \sqrt{m_i} x_i$$

If Q is normalized to 1, then the reduced mass is related by the following:

$$\mu = \frac{1}{\sum_i \frac{c_i^2}{m_i}}$$

Which is then related to the harmonic angular frequency ω and harmonic force constant k through $\omega^2 = k/\mu$.

Displacement along normal modes is done by multiplying the displacement vector q_i by a distortion scaling factor n , such that the displaced vector is defined by $(1+n)q_i$. All calculations presented here were performed between $n = -0.15$ and $n = 0.15$ in 0.05 increments to obtain coupling terms that reflective of the equilibrium geometry. For simplicity, the axes titles specify n relative to 0 and not 1, such that 0 corresponds to the equilibrium geometry.

B. Tables

Table S1a. Bond distances and angles for X-ray crystallographic and idealized D_{4h} $[\text{CuCl}_4]^{2-}$ structures.

Bond	Length (\AA) ^a	Length (\AA) ^b	Angle	Angle ($^{\circ}$) ^a	Angle ($^{\circ}$) ^b
Cu-Cl _a	2.281	2.264	Cl _a -Cu-Cl _b	89.9	90.0
Cu-Cl _b	2.247	2.264	Cl _b -Cu-Cl _c	90.2	90.0
Cu-Cl _c	2.281	2.264	Cl _c -Cu-Cl _d	89.9	90.0
Cu-Cl _d	2.247	2.264	Cl _d -Cu-Cl _a	90.2	90.0
			Cl _a -Cu-Cl _c	180.0	180.0
			Cl _b -Cu-Cl _d	180.0	180.0

^a X-ray crystal structure.⁹

^b Idealized structure from X-ray crystal structure.

Table S1b. Bond distances and angles for X-ray crystallographic and idealized D_{2d} $[\text{CuCl}_4]^{2-}$ structures. This structure was used for analysis in the main text.

Bond	Length (\AA) ^a	Length (\AA) ^b	Angle	Angle ($^{\circ}$) ^a	Angle ($^{\circ}$) ^b
Cu-Cl _a	2.189	2.208	Cl _a -Cu-Cl _b	101.3	100.1
Cu-Cl _b	2.228	2.208	Cl _b -Cu-Cl _c	98.3	100.1
Cu-Cl _c	2.189	2.208	Cl _c -Cu-Cl _d	101.3	100.1
Cu-Cl _d	2.228	2.208	Cl _d -Cu-Cl _a	98.3	100.1
			Cl _a -Cu-Cl _c	138.1	130.6
			Cl _b -Cu-Cl _d	123.1	130.6

^a X-ray crystal structure.⁹

^b Idealized structure from X-ray crystal structure.

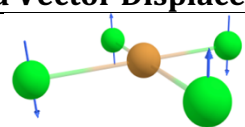
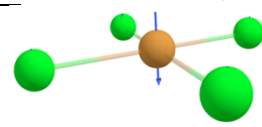
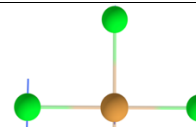
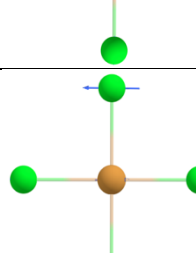
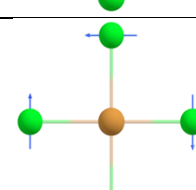
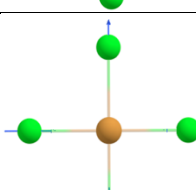
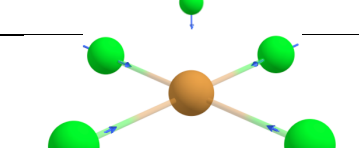
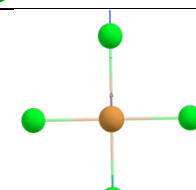
Table S1c. Bond distances and angles for a different X-ray crystallographic and idealized D_{2d} $[\text{CuCl}_4]^{2-}$ structure. g values and d-d transitions are shown for the idealized structure to emphasize similarity of values with ones used in the main text.

Bond	Length (\AA) ^a	Length (\AA) ^b	Angle	Angle ($^{\circ}$) ^a	Angle ($^{\circ}$) ^b
Cu-Cl _a	2.244	2.230	Cl _a -Cu-Cl _b	101.9	100.6
Cu-Cl _b	2.235	2.230	Cl _b -Cu-Cl _c	99.6	100.6
Cu-Cl _c	2.220	2.230	Cl _c -Cu-Cl _d	101.9	100.6
Cu-Cl _d	2.220	2.230	Cl _d -Cu-Cl _a	99.6	100.6
			Cl _a -Cu-Cl _c	131.2	129.1
			Cl _b -Cu-Cl _d	127.1	129.1
g_x^b	g_y^b	g_z^b	Assignment	Energy (cm^{-1}) ^b	
2.107	2.107	2.331	$^2\text{B}_2 \rightarrow ^2\text{E}$	6220	
				6220	
			$^2\text{B}_2 \rightarrow ^2\text{B}_1$	8310	
			$^2\text{B}_2 \rightarrow ^2\text{A}_1$	9890	

^a X-ray crystal structure.¹⁰

^b Idealized structure from X-ray crystal structure.

Table S2a. Calculated vibrational modes for idealized D_{4h} $[\text{CuCl}_4]^{2-}$, including their energies, symmetry labels, and scaled vector displacements (arrows point towards the direction of positive displacement, where $n > 0$). $\Gamma_{vib} = a_{1g} + b_{1g} + b_{2g} + a_{2u} + b_{2u} + 2e_u$

Mode #	Energy (cm ⁻¹)	Symmetry	Scaled Vector Displacements
1	-85.8	b_{2u}	
2	140.5	a_{2u}	
3	172.2	$e_u(1a)$	
4	172.2	$e_u(1b)$	
5	182.7	b_{2g}	
6	198.5	b_{1g}	
7	296.3	a_{1g}	
8	341.4	$e_u(2a)$	

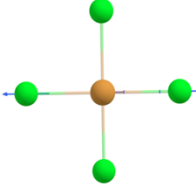
9	341.5	$e_u(2b)$	
---	-------	-----------	---

Table S2b. Calculated vibrational modes for D_{2d} $[\text{CuCl}_4]^{2-}$, including their energies, symmetry labels, and scaled vector displacements (arrows point towards the direction of positive displacement, where $n > 0$). $\Gamma_{vib} = 2a_1 + b_1 + 2b_2 + 2e$

Mode #	Energy (cm ⁻¹)	Symmetry	Scaled Vector Displacements
1	-35.5	$a_1(1)$	
2	66.9	$b_2(1)$	
3	118.3	b_1	
4	128.6	$e(1a)$	
5	128.6	$e(1b)$	
6	290.2	$b_2(2)$	
7	316.7	$a_1(2)$	
8	348.7	$e(2a)$	

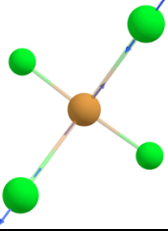
9	348.8	$e(2b)$	
---	-------	---------	---

Table S3a. Spin-phonon analyses (g_z values and ligand field energies) for idealized D_{4h} $[\text{CuCl}_4]^{2-}$.

Mode #	Energy (cm^{-1})	Symm.	Best-Fit* (g_z)*	$r^2(g_z)$	Best-Fit (${}^2\text{B}_{2g}$)*	$r^2({}^2\text{B}_{2g})$
1	-85.78	b_{2u}	$y = 0.0630x^2 + 2.2038$	1.000	$y = -3230.5x^2 + 14475.2$	1.000
2	140.47	a_{2u}	$y = 0.1185x^2 + 2.2038$	1.000	$y = -6698.1x^2 + 14475.0$	1.000
3	172.17	$e_u(1a)$	$y = -0.0559x^2 + 2.2038$	1.000	$y = -4832.4x^2 - 0.1x + 14475.0$	1.000
4	172.2	$e_u(1b)$	$y = 0.0559x^2 + 2.2038$	1.000	$y = -4839.1x^2 + 14475.0$	1.000
5	182.65	b_{2g}	$y = -0.0020x^2 + 2.2038$	0.995	$y = 112.9x^2 - 0.2x + 14475.2$	0.999
6	198.49	b_{1g}	$y = 0.0077x^2 + 2.2038$	1.000	$y = -6530.5x^2 - 0.1x + 14475.6$	1.000
7	296.29	a_{1g}	$y = -0.2411x + 2.2037$	1.000	$y = 12470.3x + 14569.2$	0.996
8	341.38	$e_u(2a)$	$y = -0.2720x^2 + 2.2038$	1.000	$y = 651.4x^2 - 0.4x + 14477.3$	0.924
9	341.51	$e_u(2b)$	$y = -0.2720x^2 + 2.2038$	1.000	$y = 660.0x^2 + 14477.3$	0.926

Quadratic equations used to fit “even” modes where $g_z(-n) = g_z(n)$. Linear equations used for fitting “odd” modes $g_z(-n) = -g_z(n)$. This has been maintained throughout the SI tables.

Table S3b. Spin–phonon analyses (g_x values and ligand field energies) for idealized D_{4h} $[\text{CuCl}_4]^{2-}$.

Mode #	Energy (cm^{-1})	Symm.	Best-Fit Equation (g_x)	$r^2 (g_x)$	Best-Fit Equation (${}^2\text{E}_g(1)$)	$r^2 ({}^2\text{E}_g(1))$
1	-85.8	b_{2u}	$y = 0.0174x^2 + 2.0555$	1.000	$y = -4393.8x^2 + 0.1x + 14608.5$	1.000
2	140.5	a_{2u}	$y = 0.0423x^2 + 2.0555$	1.000	$y = -10065.7x^2 + 14608.0$	1.000
3	172.2	$e_u(1a)$	$y = 0.0199x^2 + 2.0555$	1.000	$y = -2262.9x^2 - 0.1x + 14608.6$	1.000
4	172.2	$e_u(1b)$	$y = 0.0030x^2 + 2.0555$	0.999	$y = -3246.7x^2 + 14608.5$	1.000
5	182.7	b_{2g}	$y = 0.0049x^2 + 2.0555$	0.926	$y = -2174.3x^2 + 14600.3$	0.957
6	198.5	b_{1g}	$y = -0.0325x + 2.0555$	0.999	$y = -2409.4x - 14576.8$	0.991
7	296.3	a_{1g}	$y = -0.0724x + 2.0556$	1.000	$y = 12414.1x^2 + 14692.2$	0.997
8	341.4	$e_u(2a)$	$y = -0.0475x^2 + 2.0556$	0.999	$y = 13480.0x^2 - 0.1x + 14608.1$	1.000
9	341.5	$e_u(2b)$	$y = -0.1364x^2 + 2.0555$	1.000	$y = 3716.2x^2 + 14609.6$	0.999

Note mode 5 (b_{2g}) is V-shaped, but fitted as a quadratic function.

Table S3c. Spin–phonon analyses (g_y values and ligand field energies) for idealized D_{4h} $[\text{CuCl}_4]^{2-}$.

Mode #	Energy (cm^{-1})	Symm.	Best-Fit Equation (g_y)	r^2	Best-Fit Equation (${}^2\text{E}_g(2)$)	r^2
1	-85.8	b_{2u}	$y = 0.0174x^2 + 2.0555$	1.000	$y = -4397.1x^2 + 14608.6$	1.000
2	140.5	a_{2u}	$y = 0.0423x^2 + 2.0555$	1.000	$y = -10070.5x^2 + 14608.1$	1.000
3	172.3	$e_u(1a)$	$y = 0.0199x^2 + 2.0555$	0.999	$y = -3240.0x^2 + 14608.6$	1.000
4	172.2	$e_u(1b)$	$y = 0.0030x^2 + 2.0555$	1.000	$y = -2268.1x^2 - 0.2x + 14608.7$	1.000
5	182.7	b_{2g}	$y = -0.0050x^2 + 2.0555$	0.928	$y = 1052.4x^2 + 14616.7$	0.830
6	198.5	b_{1g}	$y = 0.0325x + 2.0555$	0.999	$y = 1986.9x + 14610.8$	0.996
7	296.3	a_{1g}	$y = -0.0724x + 2.0556$	1.000	$y = 12414.1x^2 + 14692.3$	0.997
8	341.4	$e_u(2a)$	$y = -0.1364x^2 + 2.0555$	1.000	$y = 3715.7x^2 - 0.2x + 14609.6$	0.999
9	341.5	$e_u(2b)$	$y = -0.0475x^2 + 2.0556$	0.999	$y = 13481.9x^2 + 14608.2$	1.000

Note mode 5 (b_{2g}) is V-shaped, but fitted as a quadratic function.

Table S3d. Spin-phonon analyses ($y = g_x - g_y$) for idealized D_{4h} $[\text{CuCl}_4]^{2-}$.

Mode #	Energy (cm ⁻¹)	Symm.	Best-Fit Equation (g _x - g _y)	r ²
1	-85.8	b_{2u}	$y = 0$	-
2	140.5	a_{2u}	$y = 0$	-
3	172.3	$e_u(1a)$	$y = 0.0169x^2$	1.000
4	172.2	$e_u(1b)$	$y = -0.0169x^2$	1.000
5	182.7	b_{2g}	$y = -0.0099x^2$	0.927
6	198.5	b_{1g}	$y = -0.0650x$	1.000
7	296.3	a_{1g}	$y = 0$	0.286
8	341.4	$e_u(2a)$	$y = 0.0889x^2$	0.999
9	341.5	$e_u(2b)$	$y = -0.0889x^2$	0.999

Note mode 5 (b_{2g}) is V-shaped, but fitted as a quadratic function.

Table S3e. Spin-phonon analyses (spin densities and $y = {}^2E_g(1) - {}^2E_g(2)$) for idealized D_{4h} $[\text{CuCl}_4]^{2-}$.

Mode #	Energy (cm^{-1})	Symm.	Best-Fit Equation (spin density)	r^2	Best-Fit Equation (${}^2E_g(1) - {}^2E_g(2)$)	r^2
1	-85.8	b_{2u}	$y = 0.0484x^2 + 0.6681$	1.000	$y = 3.3x^2 + 0.1x - 0.1$	0.361
2	140.5	a_{2u}	$y = -0.0265x^2 + 0.6681$	1.000	$y = 4.8x^2 - 0.1$	0.833
3	172.3	$e_u(1a)$	$y = -0.0669x^2 + 0.6681$	1.000	$y = 977.1x^2 - 0.1x$	1.000
4	172.2	$e_u(1b)$	$y = -0.0669x^2 + 0.6681$	1.000	$y = -978.6x^2 + 0.2x - 0.2$	1.000
5	182.7	b_{2g}	$y = -0.0531x^2 + 0.6681$	1.000	$y = -3226.7x^2 - 16.4$	0.922
6	198.5	b_{1g}	$y = 0.0591x^2 + 0.6681$	1.000	$y = -4396.3x - 34.0$	0.995
7	296.3	a_{1g}	$y = -0.1107x + 0.6670$	0.993	$y = -0.1$	-
8	341.4	$e_u(2a)$	$y = -0.1704x^2 + 0.6681$	0.999	$y = 9764.3x^2 + 0.1x - 1.5$	1.000
9	341.5	$e_u(2b)$	$y = -0.1704x^2 + 0.6681$	0.999	$y = -9765.7x^2 + 1.4$	1.000

Note mode 5 (b_{2g}) is V-shaped, but fitted as a quadratic function.

Table S4a. Spin-phonon analyses (g_z values and ligand field energies) for idealized D_{2d} $[\text{CuCl}_4]^{2-}$.

Mode #	Energy (cm^{-1})	Symm.	Best-Fit (g_z)	$r^2 (g_z)$	Best-Fit (${}^2\text{B}_1$)	$r^2 ({}^2\text{B}_1)$
1	-35.5	$a_1(1)$	$y = 0.1403x + 2.3098$	0.998	$y = -3923.2x + 10432.9$	1.000
2	66.9	$b_2(1)$	$y = -0.0678x^2 + 2.3090$	1.000	$y = -1477.1x^2 + 0.1x + 10439.4$	1.000
3	118.3	b_1	$y = 0.0297x^2 + 2.3090$	1.000	$y = -604.8x^2 + 10439.4$	1.000
4	128.6	$e(1a)$	$y = 0.0554x^2 + 2.3090$	1.000	$y = 481.0x^2 + 10439.6$	1.000
5	128.6	$e(1b)$	$y = 0.0554x^2 + 2.3090$	1.000	$y = 481.0x^2 + 10439.6$	1.000
6	290.2	$b_2(2)$	$y = -0.2954x^2 + 2.3090$	1.000	$y = -2764.8x^2 - 0.3x + 10439.9$	1.000
7	316.7	$a_1(2)$	$y = -0.3058x + 2.3083$	1.000	$y = 7884.4x + 10498.9$	0.996
8	348.7	$e(2a)$	$y = -0.5498x^2 + 2.3090$	1.000	$y = 7766.7x^2 + 10437.2$	0.999
9	348.7	$e(2b)$	$y = -0.5498x^2 + 2.3090$	1.000	$y = 7768.1x^2 + 0.1x + 10437.2$	0.999

Table S4b. Spin–phonon analyses (g_x values and ligand field energies) for idealized D_{2d} $[\text{CuCl}_4]^{2-}$.

Mode #	Energy (cm ⁻¹)	Symm.	Best-Fit Equation (g_x)	r ²	Best-Fit Equation (${}^2\text{E}(1)$)	r ²
1	-35.5	$a_1(1)$	$y = 0.0811x + 2.0957$	0.990	$y = -6942.4x + 6823.4$	1.000
2	66.9	$b_2(1)$	$y = -0.1697x + 2.0948$	1.000	$y = 2873.8x + 6843.1$	0.998
3	118.3	b_1	$y = -0.0735x^2 + 2.0942$	0.863	$y = -2418.0x + 6830.6$ for $x < 0$ $y = 2418.0x + 6830.6$ for $x > 0$	0.999 0.999
4	128.6	$e(1a)$	$y = -0.0424x^2 + 2.0948$	1.000	$y = -1371.4x^2 - 0.4x + 6827.5$	1.000
5	128.6	$e(1b)$	$y = 0.0628x^2 + 2.0947$	1.000	$y = -1953.3x^2 + 6827.4$	1.000
6	290.2	$b_2(2)$	$y = -0.2172x + 2.0943$	0.999	$y = 3053.1x + 6862.0$	0.991
7	316.7	$a_1(2)$	$y = -0.1519x + 2.0949$	1.000	$y = 5323.8x + 6861.9$	0.997
8	348.7	$e(2a)$	$y = -0.6174x^2 + 2.0945$	0.999	$y = 13733.3x^2 - 1.6x + 6827.1$	1.000
9	348.7	$e(2b)$	$y = 0.1079x^2 + 2.0949$	0.982	$y = 9170.5x^2 + 6830.5$	0.999

Note mode 3 (b_1) is V-shaped, but fitted as a quadratic function for $y = g_x$.

Table S4c. Spin–phonon analyses (g_y values and ligand field energies) for idealized D_{2d} $[\text{CuCl}_4]^{2-}$.

Mode #	Energy (cm^{-1})	Symm.	Best-Fit Equation (g_y)	r^2	Best-Fit Equation (${}^2\text{E}(2)$)	r^2
1	-35.5	$a_1(1)$	$y = 0.0811x + 2.0957$	0.990	$y = -6942.0x + 6823.4$	1.000
2	66.9	$b_2(1)$	$y = 0.1697x + 2.0948$	1.000	$y = -2873.1x + 6843.1$	0.998
3	118.3	b_1	$y = 0.1356x^2 + 2.0953$	0.955	$y = 2786.2x + 6830.3 \text{ for } x < 0$ $y = -2785.4x + 6412.5 \text{ for } x > 0$	1.000 1.000
4	128.6	$e(1a)$	$y = 0.0629x^2 + 2.0952$	1.000	$y = -1959.1x^2 + 6827.5$	1.000
5	128.6	$e(1b)$	$y = -0.0424x^2 + 2.0948$	1.000	$y = -1369.5x^2 + 6827.4$	1.000
6	290.2	$b_2(2)$	$y = 0.2172x + 2.0943$	0.999	$y = -3053.4x + 6862.0$	0.991
7	316.7	$a_1(2)$	$y = -0.1519x + 2.0949$	1.000	$y = 5323.5x + 6861.9$	0.997
8	348.7	$e(2a)$	$y = 0.1079x^2 + 2.0949$	0.982	$y = 9170.5x^2 + 6830.5$	0.999
9	348.7	$e(2b)$	$y = -0.6175x^2 + 2.0945$	0.999	$y = 13740.5x^2 + 0.8x + 6827.1$	1.000

Note mode 3 (b_1) is V-shaped, but fitted as a quadratic for $y = g_y$.

Table S4d. Spin-phonon analyses (g_x - g_y values) for idealized D_{2d} [CuCl₄]²⁻.

Mode #	Energy (cm ⁻¹)	Symm.	Best-Fit Equation ($g_x - g_y$)	r ²	Best-Fit Equation ² E(1) - ² E(2)	r ²
1	-35.5	$a_1(1)$	$y = -0.0000x - 0.0000$	0.0671	$y = -0.3571x - 0.0714$	0.625
2	66.9	$b_2(1)$	$y = -0.3393x + 0.0000$	1.000	$y = 5746.9x - 0.0142$	1.000
3	118.3	b_1	$y = -0.2091x^2 - 0.0010$	0.927	$y = -5203.4x + 0.2700$ for $x < 0$ $y = 5203.4x + 0.2700$ for $x > 0$	1.000 1.000
4	128.6	$e(1a)$	$y = -0.1053x^2 + 0.0000$	1.000	$y = 587.6x^2 - 0.4x + 0.0095$	1.000
5	128.6	$e(1b)$	$y = 0.1053x^2 - 0.0000$	1.000	$y = -583.8x^2 - 0.0619$	1.000
6	290.2	$b_2(2)$	$y = -0.4343x - 0.0000$	1.000	$y = 6106.4x + 0.0143$	1.000
7	316.7	$a_1(2)$	$y = 0.0000x - 0.0000$	0.197	$y = 0.2857x$	0.143
8	348.7	$e(2a)$	$y = -0.7254x^2 - 0.0004$	0.998	$y = 4562.9x^2 - 1.6x - 3.4142$	0.996
9	348.7	$e(2b)$	$y = 0.7254x^2 + 0.0004$	0.998	$y = -4570.0x^2 - 0.8x + 3.4571$	0.996

Note mode 3 (b₁) is V-shaped, but fitted as a quadratic function for $y = g_x - g_y$.

Table S4e. Spin–phonon analyses (Loewdin spin densities) for idealized D_{2d} $[\text{CuCl}_4]^{2-}$.

Mode #	Energy (cm ⁻¹)	Symm.	Best-Fit Equation (spin densities)	r ²
1	-35.5	$a_1(1)$	$y = 0.0759x + 0.7527$	1.000
2	66.9	$b_2(1)$	$y = -0.0038x^2 + 0.7525$	0.996
3	118.3	b_1	$y = -0.074x^2 + 0.7525$	1.000
4	128.6	$e(1a)$	$y = -0.0524x^2 + 0.7525$	1.000
5	128.6	$e(1b)$	$y = -0.0523x^2 + 0.7525$	1.000
6	290.2	$b_2(2)$	$y = -0.3264x^2 + 0.7525$	1.000
7	316.7	$a_1(2)$	$y = -0.1573x + 0.7510$	0.994
8	348.7	$e(2a)$	$y = -0.2429x^2 + 0.7526$	0.999
9	348.7	$e(2b)$	$y = -0.2429x^2 + 0.7526$	0.999

Table S5. Bond distances and angles for X-ray crystallographic and idealized C_{4v} $[\text{VOCl}_4]^{2-}$ structures.

	Crystal Structure ¹¹	Idealized Structure
V–O bond length (Å)	1.580	1.580
V–Cl _a bond length (Å)	2.362	2.354
V–Cl _b bond length (Å)	2.370	2.354
V–Cl _c bond length (Å)	2.327	2.354
V–Cl _d bond length (Å)	2.358	2.354
O–V–Cl _a bond angle (°)	106.7	104.3
O–V–Cl _b bond angle (°)	101.7	104.3
O–V–Cl _c bond angle (°)	107.4	104.3
O–V–Cl _d bond angle (°)	101.5	104.3
Cl _a –V–Cl _b bond angle (°)	85.6	86.5
Cl _a –V–Cl _c bond angle (°)	145.9	151.4
Cl _a –V–Cl _d bond angle (°)	87.7	86.5
Cl _b –V–Cl _c bond angle (°)	86.3	86.5
Cl _b –V–Cl _d bond angle (°)	156.9	151.4
Cl _c –V–Cl _d bond angle (°)	87.0	86.5

Table S6. Calculated vibrational modes for idealized C_{4v} $[\text{VOCl}_4]^{2-}$, including their energies, symmetry labels, and scaled vector displacements (arrows point towards the direction of positive displacement, where $n > 0$). $\Gamma_{\text{vib}} = 3a_1 + 2b_1 + b_2 + 3e$

Mode #	Energy (cm ⁻¹)	Symmetry	Scaled Vector Displacements
1	-51.3	$b_1(1)$	
2	160.3	$e(1a)$	
3	160.3	$e(1b)$	
4	166.4	$a_1(1)$	
5	186.8	b_2	
6	233.2	$b_1(2)$	
7	267.1	$e(2a)$	
8	267.1	$e(2b)$	

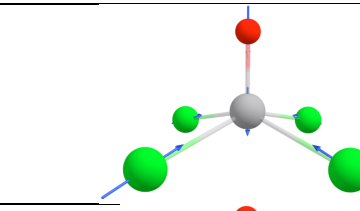
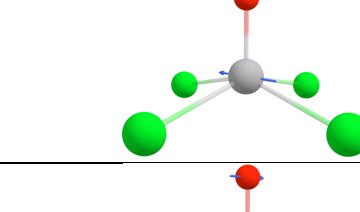
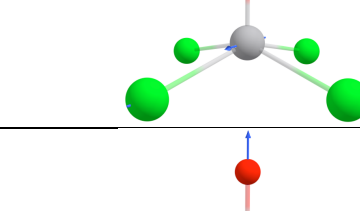
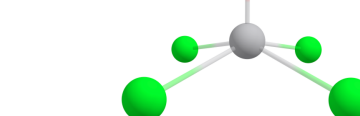
9	323.5	$a_1(2)$	
10	394.9	$e(3a)$	
11	394.9	$e(3b)$	
12	1050.4	$a_1(3)$	

Table S7a. Spin–phonon analyses (g_z values and ligand field energies) for idealized C_{4v} $[\text{VOCl}_4]^{2-}$.

Mode #	Energy (cm^{-1})	Symm.	Best-Fit (g_z)	$r^2(g_z)$	Best-Fit (${}^2\text{B}_1$)	$r^2({}^2\text{B}_1)$
1	-51.3	$b_1(1)$	$y = -0.0162x^2 + 1.9628$	1.000	$y = -3545.7x^2 + 15227.9$	1.000
2	160.3	$e(1a)$	$y = -0.0202x^2 + 1.9628$	1.000	$y = -5094.3x^2 + 15227.5$	1.000
3	160.3	$e(1b)$	$y = -0.0202x^2 + 1.9628$	1.000	$y = -5094.3x^2 + 15227.5$	1.000
4	166.4	$a_1(1)$	$y = -0.0183x^2 + 0.0020x + 1.9628$	1.000	$y = -3576.2x^2 - 298.857x + 15227.9$	1.000
5	186.8	b_2	$y = -0.0049x^2 + 1.9628$	1.000	$y = -564.8x^2 + 15228.0$	1.000
6	233.1	$b_1(2)$	$y = -0.0164x^2 + 1.9628$	1.000	$y = -10295.2x^2 + 15227.7$	1.000
7	267.1	$e(2a)$	$y = 0.0171x^2 + 1.9628$	1.000	$y = 1369.5x^2 + 15228.6$	0.998
8	267.1	$e(2b)$	$y = 0.0171x^2 + 1.9628$	1.000	$y = 1369.5x^2 + 15228.6$	0.998
9	323.5	$a_1(2)$	$y = 0.0684x + 1.9626$	1.000	$y = 13943.1x + 15312.6$	0.997
10	394.9	$e(3a)$	$y = -0.3125x^2 + 1.9626$	0.998	$y = -91921.0x^2 + 15002.2$	0.974
11	394.9	$e(3b)$	$y = -0.3125x^2 + 1.9626$	0.997	$y = -91921.0x^2 - 0.1x + 15002.2$	0.974
12	1050.4	$a_1(3)$	$y = 0.0302x + 1.9628$	0.999	-	-

Table S7b. Spin–phonon analyses (g_x values and ligand field energies) for idealized C_{4v} $[\text{VOCl}_4]^{2-}$.

Mode #	Energy (cm ⁻¹)	Symm.	Best-Fit (g_x)	r ² (g_x)	Best-Fit (2E(1))	r ² (2E(1))
1	-51.3	$b_1(1)$	y = -0.0022x + 1.9730	1.000	y = -1951.0x + 16333.9	0.998
2	160.3	$e(1a)$	y = -0.0044x ² + 1.9730	1.000	y = 1278.1x ² + 16325.1	0.999
3	160.3	$e(1b)$	y = 0.0029x ² + 1.9730	1.000	y = -844.8x ² + 16324.6	1.000
4	166.4	$a_1(1)$	y = -0.0069x + 1.9730	1.000	y = -2118.9x + 16341.0	0.996
5	186.8	b_2	y = -0.0030x + 1.9730 for x<0 y = 0.0030x + 1.9730 for x>0	1.000 1.000	y = -648.2x + 16232.4 for x<0 y = 648.2x + 16232.4 for x>0	0.999 0.999
6	233.1	$b_1(2)$	y = -0.0017x + 1.9730	0.993	y = -3227.6x ² + 16287.6	0.990
7	267.1	$e(2a)$	y = -0.0313x ² + 1.9730	1.000	y = -5947.6x ² + 16324.5	1.000
8	267.1	$e(2b)$	y = -0.0331x ² + 1.9730	1.000	y = -9620.0x ² + 16323.7	1.000
9	323.5	$a_1(2)$	y = 0.0047x + 1.9729	0.988	y = -3539.1x + 16312.5	0.999
10	394.9	$e(3a)$	y = 0.1276x ² + 1.9732	0.983	y = 70592.4x ² + 16551.2	0.957
11	394.9	$e(3b)$	y = -0.0533x ² + 1.9730	0.999	y = -20075.2x ² - 0.1x + 16323.1	0.957
12	1050.4	$a_1(3)$	y = -0.1014x + 1.9739	0.979		0.998

Table S7c. Spin–phonon analyses (g_y values and ligand field energies) for idealized C_{4v} $[\text{VOCl}_4]^{2-}$.

Mode #	Energy (cm^{-1})	Symm.	Best-Fit Equation (g_y)	$r^2 (g_y)$	Best-Fit Equation (${}^2\text{E}(2)$)	$r^2 ({}^2\text{E}(2))$
1	-51.3	$b_1(1)$	$y = 0.0022x + 1.9730$	1.000	$y = 1951.0x + 16333.9$	0.998
2	160.3	$e(1a)$	$y = 0.0029x^2 + 1.9730$	1.000	$y = -844.8x^2 + 16324.6$	1.000
3	160.3	$e(1b)$	$y = -0.0044x^2 + 1.9730$	1.000	$y = 1278.1x^2 + 16325.1$	0.999
4	166.4	$a_1(1)$	$y = -0.0069x + 1.9730$	1.000	$y = 1633.8x^2 - 2119.1x + 16324.6$	1.000
5	186.8	b_2	$y = 0.0031x + 1.9730 \text{ for } x < 0$ $y = -0.0031x + 1.9730 \text{ for } x > 0$	1.000 1.000	$y = 488.6x + 16323.2 \text{ for } x < 0,$ $y = -488.6x + 16323.2 \text{ for } x > 0$	0.997 0.997
6	233.1	$b_1(2)$	$y = 0.0017x + 1.9730$	0.993	$y = 3227.6x + 16287.6$	0.990
7	267.1	$e(2a)$	$y = -0.0331x^2 + 1.9730$	1.000	$y = -9620.0x^2 + 16323.7$	1.000
8	267.1	$e(2b)$	$y = -0.0313x^2 + 1.9730$	1.000	$y = -5947.6x^2 + 16324.5$	1.000
9	323.5	$a_1(2)$	$y = 0.0047x + 1.9729$	0.988	$y = -3539.1x + 16312.5$	0.999
10	394.9	$e(3a)$	$y = -0.0533x^2 + 1.9730$	0.999	$y = -20075.2x^2 + 16323.2$	0.999
11	394.9	$e(3b)$	$y = 0.1276x^2 + 1.9732$	0.983	$y = 70592.4x^2 + 16551.2$	0.957
12	1050.4	$a_1(3)$				

Table S7d. Spin-phonon analyses ($y = g_x - g_y$ and $y = {}^2E(1) - {}^2E(2)$) for idealized C_{4v} [VOCl₄]²⁻

Mode #	Energy (cm ⁻¹)	Symm.	Best-Fit Equation (g _x - g _y)	r ² (g _x - g _y)	Best-Fit Equation ({} ² E(1) - {} ² E(2))	r ² ({} ² E(1) - {} ² E(2))
1	-51.3	<i>b</i> ₁ (1)	$y = -0.0044x^2$	1.000	$y = -3902.0x^2$	1.000
2	160.3	<i>e</i> (1 <i>a</i>)	$y = -0.0073x^2$	1.000	$y = 2122.9x^2 - 0.5$	1.000
3	160.3	<i>e</i> (1 <i>b</i>)	$y = 0.0073x^2$	1.000	$y = -2122.9x^2 - 0.4$	1.000
4	166.4	<i>a</i> ₁ (1)	$y = 0$	-	$y = 0.1x$	0.167
5	186.8	<i>b</i> ₂	$y = -0.0060x + 0.0000$ for $x < 0$, $y = 0.0060 + 0.0000$ for $x > 0$	1.000 1.000	$y = -1136.8x + 0.1$ for $x < 0$, $y = 1136.8x + 0.1$ for $x > 0$	1.000 1.000
6	233.1	<i>b</i> ₁ (2)	$y = -0.003x$	1.000	$y = -6455.3x^2$	1.000
7	267.1	<i>e</i> (2 <i>a</i>)	$y = 0.0018x^2$	1.000	$y = 3672.4x^2 + 0.8$	1.000
8	267.1	<i>e</i> (2 <i>b</i>)	$y = -0.0018x^2$	1.000	$y = -3672.4x^2 - 0.8$	1.000
9	323.5	<i>a</i> ₁ (2)	$y = 0$	-	$y = 0$	-
10	394.9	<i>e</i> (3 <i>a</i>)	$y = 0.1809x^2 + 0.0002$	0.992	$y = 90667.6x^2 + 228.0$	0.973
11	394.9	<i>e</i> (3 <i>b</i>)	$y = -0.1809x^2 - 0.0002$	0.992	$y = -90667.6x^2 - 0.1x - 228.0$	0.973
12	1050.4	<i>a</i> ₁ (3)	$y = 0$	-		

Table S7e. Spin–phonon analyses (Loewdin spin densities) for idealized C_{4v} [VOCl₄]²⁻.

Mode #	Energy (cm ⁻¹)	Symm.	Best-Fit Equation (spin densities)	r ²
1	-51.3	<i>b</i> ₁ (1)	y = 0.0055x ² + 0.9828	1.000
2	160.3	<i>e</i> (1 <i>a</i>)	y = 0.0114x ² + 0.9828	1.000
3	160.3	<i>e</i> (1 <i>b</i>)	y = 0.0114 ² - 0.0131x + 0.9828	1.000
4	166.4	<i>a</i> ₁ (1)	y = 0.0349x ² - 0.0131x + 0.9828	1.000
5	186.8	<i>b</i> ₂	y = 0.0236x ² + 0.9828	1.000
6	233.1	<i>b</i> ₁ (2)	y = -0.1498x ² + 0.9828	1.000
7	267.1	<i>e</i> (2 <i>a</i>)	y = -0.0112x ² + 0.9828	1.000
8	267.1	<i>e</i> (2 <i>b</i>)	y = -0.0112x ² + 0.9828	1.000
9	323.5	<i>a</i> ₁ (2)	y = -0.1024x + 0.9823	0.999
10	394.9	<i>e</i> (3 <i>a</i>)	y = -0.2412x ² + 0.9828	0.999
11	394.9	<i>e</i> (3 <i>b</i>)	y = -0.2412x ² + 0.9828	0.999
12	1050.4	<i>a</i> ₁ (3)	-	-

Table S8a. Spin-phonon analysis for CuPc.

Mode #	Energy (cm ⁻¹)	Best-Fit Equation (g _z)	r ²
1	21.3*	y = 0.0001x ² + 2.1634	0.995
2	36.9	y = 0.0005x ² + 2.1634	>0.999
3	57.6	y = 0.000006x ² + 2.1634	0.462
4	65.5	y = 0.0014x ² + 2.1634	>0.999
5	65.6	y = 0.0014x ² + 2.1634	>0.999
6	114.6	y = 0.0002x ² + 2.1634	0.988
7	122.4	y = -0.0000x ² + 2.1634	0.955
8	122.4	y = -0.0000x ² + 2.1634	0.910
9	124.7	y = 0.0000x ² + 2.1634	0.858
10	128.5	y = 0.0010x ² + 2.1634	>0.999
11	128.5	y = 0.0010x ² + 2.1634	>0.999
12	143.1*	y = 0.0039x ² + 2.1634	>0.999
13	151.7	y = 0.0158x ² + 2.1634	>0.999
14	173.8	y = -0.0017x ² + 2.1634	>0.999
15	219.3	y = 0.0015x ² + 2.1634	>0.999
16	230.3	y = -0.0000x ² + 2.1634	0.953
17	239.4	y = 0.0039x ² + 2.1634	>0.999
18	256.6	y = 0.0076x ² + 2.1634	>0.999
19	256.7	y = 0.0076x ² + 2.1634	>0.999
20	259.4**	y = 0.0404x + 2.1634	>0.999
21	282.2*	y = 0.0173x ² + 2.1634	>0.999
22	288.2	y = 0.0196x ² + 2.1634	>0.999
23	292.4	y = 0.0299x ² + 2.1634	>0.999
24	292.9	y = 0.0297x ² + 2.1634	>0.999
25	298.5	y = 0.0069x ² + 2.1634	>0.999
26	298.6	y = 0.0069x ² + 2.1634	>0.999
27	308.5	y = -0.0134x ² + 2.1634	>0.999
28	308.8	y = -0.0142x ² + 2.1634	>0.999
29	367.9	y = 0.0101x ² + 2.1634	>0.999

* B_{2u} parent mode** A_{1g} parent mode

Table S8b. Spin-phonon analyses for [Cu(mnt)₂]²⁻.

Mode #	Energy (cm ⁻¹)	Best-Fit Equation (g _z)	r ²
1*	43.1	y = 0.0036x ² + 2.0849	>0.999
2	45.5	y = 0.0004x ² + 0.0003x + 2.0849	>0.999
3	53.8	y = 0.0016x ² - 0.0007x + 2.0849	>0.999
4	57.7	y = 0.0023x ² + 2.0849	>0.999
5	63.5	y = 0.0009x ² + 2.0849	>0.999
6	72.0	y = 0.0156x ² - 0.0025x + 2.0849	>0.999
7*	93.8	y = -0.0024x ² + 2.0849	>0.999
8	99.2	y = 0.0008x ² + 0.0007x + 2.0849	>0.999
9	120.1	y = -0.0010x ² + 0.0141x + 2.0849	>0.999
10	131.7	y = -0.0001x ² + 2.0849	0.991
11	134.4	y = -0.0043x ² - 0.0050x + 2.0849	>0.999
12	141.2	y = 0.0379x ² + 2.0849	>0.999
13	154.3	y = -0.0028x ² + 0.0147x + 2.0849	>0.999
14	188.4	y = 0.0035x ² + 2.0849	>0.999
15	215.4	y = 0.0090x ² + 2.0849	>0.999
16	218.0	y = -0.0013x ² + 0.0009x + 2.0849	>0.999
17	222.9	y = -0.0151x ² + 0.0041x + 2.0849	>0.999
18	226.7	y = -0.0011x ² + 2.0849	>0.999
19	287.8	y = -0.0932x ² - 0.0001x + 2.0849	>0.999
20**	303.4	y = -0.1118x + 2.0848	>0.999
21	306.2	y = -0.1261x ² + 0.0014x + 2.0849	>0.999
22	398.1	y = -0.0002x ² + 0.0019x + 2.0849	>0.999
23	405.5	y = -0.0177x ² + 2.0849	>0.999
24	409.1	y = -0.0286x ² + 0.0009x + 2.0849	>0.999
25	412.3	y = -0.0157x ² + 2.0849	>0.999

Note modes 2 and 3 are rotational motions, not intramolecular vibrations.

* B_{2u} parent mode

** A_{1g} parent mode

Table S8c. Spin-phonon analyses for $[\text{Cu}(\text{bdt})_2]^{2-}$.

Mode #	Energy (cm^{-1})	Best-Fit Equation (g_z)	r^2
1*	-104.1	$y = 0.0068x^2 + 2.0467$	>0.999
2	-87.2	$y = 0.0081x^2 - 0.0017x + 2.0467$	>0.999
3	-49.4	$y = 0.0001x^2 + 2.0467$	0.969
4	51.3	$y = 0.0009x^2 + 2.0467$	>0.999
5	85.1	$y = 0.0465x^2 + 2.0467$	>0.999
6*	108.0	$y = -0.0016x^2 + 2.0467$	>0.999
7	115.1	$y = -0.0017x^2 + 2.0467$	>0.999
8	179.8	$y = -0.0001x^2 - 0.0107x + 2.0467$	>0.999
9	206.2	$y = 0.0008x^2 + 2.0467$	>0.999
10	219.1	$y = 0.0024x^2 - 0.0015x + 2.0467$	>0.999
11	233.6	$y = 0.0004x^2 + 2.0467$	>0.999
12	246.6	$y = 0.0321x^2 + 2.0467$	>0.999
13	298.3	$y = 0.0017x^2 + 2.0467$	>0.999
14	382.2	$y = -0.0074x^2 + 0.0076x + 2.0467$	>0.999
15**	387.4	$y = -0.0920x + 2.0468$	>0.999

* B_{2u} parent mode** A_{1g} parent mode

Table S8d. Spin-phonon analyses for $[\text{Cu}(\text{bds})_2]^{2-}$.

Mode #	Energy (cm⁻¹)	Best-Fit Equation (g_z)	r²
1*	-61.7	y = 0.0005x ² + 2.0893	0.997
2	-35.0	y = 0.0003x ² - 0.0004x + 2.0893	>0.999
3	-29.6	y = -0.0000x ² + 2.0893	0.941
4	31.6	y = 0.0011x ² + 2.0893	>0.999
5	58.0	y = 0.0000x ² - 0.0003x + 2.0893	>0.999
6*	58.4	y = 0.0013x ² + 2.0893	>0.999
7	97.8	y = 0.0312x ² + 2.0893	>0.999
8	103.5	y = -0.0004x ² - 0.0080x + 2.0893	>0.999
9	107.4	y = -0.0006x ² - 0.0051x + 2.0893	>0.999
10	156.8	0.0033x ² + 2.0893	0.998
11	187.1	0.0036x ² - 0.0027x + 2.0893	>0.999
12	197.7	0.0007x ² + 0.0001x + 2.0893	>0.999
13**	199.3	y = -0.0615x + 2.0893	>0.999
14	222.1	y = 0.0046x ² + 2.0893	>0.999
15	244.7	y = 0.0026x ² - 0.0015x + 2.0893	>0.999
16	253.8	y = -0.0791x ² + 2.0893	>0.999
17	281.8	y = -0.0329x ² + 2.0893	>0.999
18	363.5	y = -0.0207x ² + 0.0020x + 2.0893	>0.999
19	373.4	y = -0.0146x ² + 2.0893	>0.999
20	373.7	y = 0.0054x ² + 0.0032x + 2.0893	>0.999
21	375.7	y = -0.0073x ² + 2.0893	>0.999

* B_{2u} parent mode** A_{1g} parent mode

Table S9a. Spin–phonon analyses for VOPc.

Mode #	Energy (cm ⁻¹)	Best-Fit Equation (g _z)	r ²
1	21.5	y = -0.0000x ² + 1.9609	0.702
2	41.5	y = -0.0007x + 1.9609	>0.999
3	58.8	y = -0.0000x + 1.9609	0.931
4	64.6	y = -0.0004x ² + 1.9609	0.998
5	64.7	y = -0.0004x ² + 1.9609	>0.999
6	117.9	y = -0.00008x ² + 1.9609	0.927
7	121.3	y = -0.0001x ² + 1.9609	0.957
8	121.3	y = -0.0001x ² + 1.9609	0.960
9	127.5	y = 0.0000x ² + 1.9609	0.866
10	130.2	y = -0.0003x ² + 1.9609	0.981
11	130.2	y = -0.0003x ² + 1.9609	0.993
12	148.5	y = -0.0011x ² + 1.9609	>0.999
13*	177.3	y = -0.0088x + 1.9609	>0.999
14	180.9	y = -0.0013x ² + 1.9609	>0.999
15	180.9	y = -0.0013x ² + 1.9609	>0.999
16	186.6	y = -0.0003x ² + 1.9609	0.991
17	226.5	y = -0.0003x ² + 1.9609	>0.999
18	232.2	y = -0.0003x ² + 1.9609	0.995
19	248.1	y = -0.0012x ² + 1.9609	0.997
20**	260.0	y = -0.0062x + 1.9609	>0.999
21	277.1	y = -0.0006x ² + 1.9609	0.989
22	277.1	y = -0.0005x ² + 1.9609	0.996
23	306.4	y = -0.0018x ² + 0.0001x + 1.9609	0.924
24	306.4	y = -0.0018x ² - 0.0001x + 1.9609	0.932
25	314.1	y = -0.0039x ² + 1.9609	>0.999
26*	317.3	y = -0.0143x + 1.9608	>0.999
27	332.4	y = -0.0003x ² + 1.9609	0.996
28	332.5	y = 0.0002x + 1.9609	0.987
29***	384.2	y = -0.0632x ² - 0.0001x + 1.9609	>0.999
30***	384.2	y = -0.0593x ² + 1.9609	>0.999
31*	393.9	y = -0.0173x + 1.9608	>0.999

* Significant pyramidal bending character

** Significant M-L stretching character (with ligands other than oxo)

*** Significant V movement in the equatorial ligand plane

Table S9b. Spin-phonon analyses for VO(acac)₂.

Mode #	Energy (cm ⁻¹)	Best-Fit Equation (g _z)	r ²
1	30.1	y = -0.0005x ² + 1.9454	>0.999
2	42.0	y = -0.0003x ² + 0.0008x - 1.9454	>0.999
3	76.1	y = -0.0006x ² + 1.9454	>0.999
4	82.1	y = -0.0004x ² + 1.9454	>0.999
5	90.7	y = 0.0000x ² + 1.9454	0.998
6	97.0	y = -0.0006x ² + 1.9454	>0.999
7	101.8	y = 0.0000x ² + 1.9454	0.203
8	103.3	y = -0.0000x ² + 1.9454	0.997
9	138.1	y = -0.0009x ² + 1.9454	>0.999
10	143.9	y = -0.0028x ² + 1.9454	>0.999
11	168.7	y = -0.0000x ² - 0.0001x + 1.9454	>0.999
12	169.3	y = -0.0004x + 1.9454	>0.999
13*	192.3	y = 0.0060x + 1.9454	>0.999
14	231.0	y = -0.0023x ² + 0.0002x + 1.9454	>0.999
15	243.0	y = -0.0010x ² + 1.9454	>0.999
16	253.3	y = -0.0034x ² + 1.9454	>0.999
17	267.1	y = -0.0010x ² - 0.0001x + 1.9454	>0.999
18	277.6	y = -0.0020x ² + 0.0057x + 1.9454	>0.999
19**	295.6	y = -0.0089x ² - 0.0214x + 1.9454	>0.999
20***	374.5	y = -0.0286x ² - 0.0001x + 1.9454	>0.999
21***	391.0	y = -0.0299x ² - 0.0002x + 1.9454	>0.999

* Significant pyramidal bending character.

** Significant M-L stretching character (with ligands other than oxo).

*** Significant V movement in the equatorial ligand plane.

Table S9c. Spin-phonon analyses for $[VO(\text{cat})_2]^{2-}$.

Mode #	Energy (cm^{-1})	Best-Fit Equation (g_z)	r^2
1	32.6	$y = -0.0004x + 1.9613$	0.999
2	53.7	$y = -0.0016x^2 - 1.9513$	>0.999
3	82.7	$y = -0.0035x^2 + 1.9513$	>0.999
4	84.6	$y = -0.0010x^2 + 1.9513$	>0.999
5	179.3	$y = 0.0002x^2 + 1.9513$	0.988
6**	186.1	$y = -0.0042x + 1.9512$	0.996
7	197.8	$y = -0.0015x^2 - 0.0001x + 1.9513$	>0.999
8	228.3	$y = -0.0012x^2 + 1.9513$	0.999
9	254.0	$y = -0.0014x^2 - 0.0003x + 1.9513$	>0.999
10	269.0	$y = -0.0011x^2 + 1.9513$	0.998
11*	280.1	$y = -0.0168x + 1.9512$	>0.999
12	340.9	$y = -0.0011x^2 + 1.9513$	>0.999
13*	366.3	$y = -0.0115x + 1.9512$	0.998
14***	388.4	$y = -0.0387x^2 + 1.9513$	>0.999
15***	437.4	$y = -0.0655x^2 + 1.9513$	0.999

* Significant pyramidal bending character

** Significant M-L stretching character (with ligands other than oxo)

*** Significant V movement in the equatorial ligand plane

Table S9d. Spin–phonon analyses for [VO(dmit)₂]²⁻.

Mode #	Energy (cm ⁻¹)	Best-Fit Equation (g _z)	r ²
1	-42.0	y = -0.0076x ² + 1.9634	>0.999
2	-22.7	y = -0.0024x ² + 0.0003x - 1.9634	>0.999
3	9.3	y = -0.0036x ² - 0.0010x + 1.9634	>0.999
4	51.6	y = -0.0017x ² + 1.9634	>0.999
5	87.2	y = -0.0020x ² + 1.9634	>0.999
6	92.6	y = -0.0002x ² - 0.0001x + 1.9634	>0.999
7	116.8	y = -0.0024x ² - 0.0030x + 1.9634	>0.999
8	120.7	y = 0.0003x ² + 0.0014x + 1.9634	>0.999
9	127.2	y = 0.0004x ² + 1.9634	>0.999
10	144.6	y = -0.0002x ² - 0.0006x + 1.9634	>0.999
11	175.8	y = -0.0010x ² + 1.9634	>0.999
12	178.6	y = -0.0160x + 1.9632	0.993
13	189.0	y = -0.0049x ² + 1.9634	>0.999
14	256.5	y = -0.0005x ² + 1.9634	0.998
15	261.5	y = 0.0017x ² + 1.9634	>0.999
16	261.9	y = -0.0110x ² + 0.0006x + 1.9634	>0.999
17*	276.9	y = 0.00481x + 1.9634	>0.999
18	302.6	y = -0.0024x ² + 1.9634	>0.999
19	330.2	y = -0.0128x ² + 1.9634	>0.999
20	349.0	y = -0.0134x ² + 1.9634	>0.999
21**	350.7	y = -0.0430x + 1.9633	>0.999
22	356.7	y = -0.0045x ² + 0.0017x + 1.9634	>0.999
23**	378.5	y = 0.0313x + 1.9633	>0.999
24	414.0	y = -0.0222x ² + 1.9634	>0.999
25	415.9	y = -0.0078x ² - 0.0009x + 1.9634	>0.999
26***	426.6	y = -0.0580x ² + 1.9634	>0.999
27***	442.7	y = -0.0267x ² + 1.9634	>0.999

* Significant pyramidal bending character

** Significant M-L stretching character (with ligands other than oxo)

*** Significant V movement in the equatorial ligand plane

Table S9e. Spin-phonon analyses for $[V(bdt)_3]^{2-}$.

Mode #	Energy (cm ⁻¹)	Best-Fit Equation (g _z)	r ²
1	16.5	y = -0.0003x + 1.9629	0.990
2	24.7	y = 0.0014x ² + 0.0001x + 1.9628	0.721
3	39.3	y = -0.0003x + 1.9628	0.941
4	59.9	y = -0.0015x ² + 1.9629	0.978
5	66.7	y = -0.0014x + 1.9628	0.987
6	74.3	y = 0.0013x + 1.9628	0.994
7	115.6	y = -0.0006x ² - 0.0001x + 1.9629	0.969
8	123.6	y = -0.0021x + 1.9629	0.981
9	136.5	y = 0.0020x + 1.9628	>0.999
10	150.1	y = -0.0045x + 1.9624	>0.999
11	152.4	y = -0.0008x + 1.9628	0.998
12	156.2	y = -0.0042x + 1.9628	0.992
13	181.2	y = 0.0013x + 1.9628	0.992
14	192.4	y = 0.0017x + 1.9629	0.971
15	195.6	y = -0.0011x + 1.9629	0.918
16	251.6	y = 0.0075x ² - 0.0005x + 1.9629	>0.999
17	255.2	y = 0.0064x ² + 0.0015x + 1.9628	>0.999
18	264.6	y = 0.0012x + 1.9629	0.925
19	284.5	y = 0.0091x + 1.9630	0.969
20	289.3	y = 0.0270x ² - 0.0064x + 1.9629	>0.999
21	301.3	y = 0.0102x ² + 0.0009x + 1.9629	>0.999
22*	351.7	y = -0.1165x + 1.9610	0.987
23	355.0	y = -0.0425x + 1.9627	>0.999
24	368.0	y = -0.0308x + 1.9628	>0.999
25	391.9	y = 0.0228x ² - 0.0046x + 1.9628	0.997
26	393.6	y = 0.0107x ² + 0.0021x + 1.9628	>0.999

* Symmetric M-L stretching mode

Table S9f. Spin-phonon analyses for [V(bds)₃]²⁻.

Mode #	Energy (cm ⁻¹)	Best-Fit Equation (g _z)	r ²
1	12.1	y = -0.0051x ² + 0.0001x + 1.8512	0.984
2	17.4	y = -0.0102x + 1.8512	0.997
3	32.2	y = -0.0025x ² - 0.0001x + 1.8512	0.982
4	48.0	y = -0.0042x ² - 0.0002x + 1.8512	0.991
5	51.5	y = -0.0117x + 1.8511	0.996
6	61.9	y = 0.0137x + 1.8511	0.996
7	81.3	y = -0.0668x ² - 0.0059x + 1.8514	0.910
8	84.6	y = -0.0283x ² + 1.8512	0.999
9	95.7	y = -0.0156x ² + 0.0001x + 1.8512	0.999
10	124.1	y = -0.0244x + 1.8510	0.995
11	138.5	y = -0.0096x ² - 0.0006x + 1.8512	0.999
12	138.8	y = 0.0079x + 1.8512	0.999
13	142.5	y = -0.0282x ² + 0.0017x + 1.8512	0.997
14	144.1	y = -0.0172x ² + 0.0001x + 1.8512	0.999
15	147.5	y = -0.0174x + 1.8512	0.999
16	180.9	y = -0.2711x ² - 0.0102 + 1.8509	0.987
17	182.8	y = -0.2562x ² - 0.0001x + 1.8510	0.996
18*	209.8	y = 0.6262x + 1.8310	0.919
19	227.2	y = -0.0095x ² + 1.8512	0.998
20	238.5	y = -0.0137x + 1.8511	0.987
21	242.2	y = -0.0031x ² - 0.0001x + 1.8512	0.995
22	251.0	y = -0.0154x ² + 1.8512	0.999
23	261.2	y = -0.0332x ² - 0.0057x - 1.8512	0.999
24	263.1	y = 0.0003x ² - 0.0001x + 1.8517	0.924
25	302.8	y = -1.2173x ² + 0.0741x + 1.8503	0.987
26	319.8	y = -0.5816x ² - 0.0001x + 1.8517	0.996
27	325.4	y = 0.0418x ² + 1.8513	0.942
28	380.8	y = 0.0914x + 1.8506	0.997
29	381.8	y = -0.0346x + 1.8510	0.996
30	382.6	y = -0.0176x ² - 0.0001x + 1.8512	0.999
31	397.1	y = -0.0200x ² + 1.8512	0.999
32	399.8	y = -0.0237x ² - 0.0040x + 1.8512	0.999

* Symmetric M-L stretching mode

Table S10a. Comparisons between optimized and X-ray crystal structure of CuPc.

	Cu-N ₁ (Å)	Cu-N ₂ (Å)	Cu-N ₃ (Å)	Cu-N ₄ (Å)
Experimental ¹²	1.960	1.965	1.960	1.965
Computed (optimized)	1.968	1.970	1.968	1.970
Difference	0.008	0.005	0.002	0.005

Table S10b. Comparisons between optimized and X-ray crystal structure of CuN₄ complexes.

R = H	Dihedral Angle (°) ^a	Cu-N ₁ (Å)	Cu-N ₁ (Å)	Cu-N ₁ (Å)	Cu-N ₁ (Å)
Experimental ¹³	0	1.950	1.950	1.971	1.971
Computed (optimized)	6.5	1.994	1.994	2.043	2.043
R = Me	Dihedral Angle (°)	Cu-N ₁ (Å)	Cu-N ₁ (Å)	Cu-N ₁ (Å)	Cu-N ₁ (Å)
Experimental ¹³	32-33	1.938	1.938	2.016	2.016
Computed (optimized)	30.5	1.983	1.984	2.081	2.082
R = tert-Bu	Dihedral Angle (°)	Cu-N ₁ (Å)	Cu-N ₁ (Å)	Cu-N ₁ (Å)	Cu-N ₁ (Å)
Experimental ¹³	61	1.937	1.937	2.057	2.057
Computed (optimized)	55.6	1.966	1.966	2.136	2.136

^a Dihedral angle defined as the dihedral angle between the two chelating N(imine)-Cu-N(pyrrolate) planes.

Table S11a. Comparisons between optimized and X-ray crystal structure of VOPc.

	Crystal structure ¹²	DFT optimized structure
V-N ₁ (Å)	2.023	2.058
V-N ₂ (Å)	2.019	2.058
V-N ₃ (Å)	2.033	2.058
V-N ₄ (Å)	2.032	2.058
V-O (Å)	1.599	1.554
O-V-N ₁ (°)	106.2	108.0
O-V-N ₂ (°)	104.6	108.1
O-V-N ₃ (°)	106.0	108.0
O-V-N ₄ (°)	106.3	107.9

Table S11b. Comparisons between optimized and X-ray crystal structure of [VO(cat)₂]²⁻.

	Crystal structure ¹⁴	DFT optimized structure
V-O ₁ (Å)	1.960	1.996
V-O ₂ (Å)	1.978	1.999
V-O ₃ (Å)	1.973	1.996
V-O ₄ (Å)	1.980	1.999
V=O (Å)	1.614	1.584
O-V-N ₁ (°)	110.4	109.0
O-V-N ₂ (°)	108.0	108.9
O-V-N ₃ (°)	109.2	109.0
O-V-N ₄ (°)	105.6	108.9

Table S11c. Comparisons between optimized and X-ray crystal structure of VO(acac)₂.

	Crystal Structure ¹⁵	DFT optimized structure
V-O ₁ (Å)	1.957	1.996
V-O ₂ (Å)	1.973	1.996
V-O ₃ (Å)	1.978	1.997
V-O ₄ (Å)	1.960	1.997
V=O (Å)	1.558	1.549
O-V-N ₁ (°)	106.3	107.7
O-V-N ₂ (°)	104.5	107.8
O-V-N ₃ (°)	108.2	107.7
O-V-N ₄ (°)	105.6	107.9

Table S12. Spin–phonon coupling terms across a variety of V(IV) complexes.

Complex	Mode (cm⁻¹)	(g_z/Q_i)	ES^a	M(d)^b	M SD
<i>C</i> _{4v} [VOCl ₄] ²⁻	166.4	-0.018	15230	88 %	0.983
	323.5	0.068			
	394.9	-0.313			
	394.9	-0.322			
VOPc	177.3	-0.009	22745	85 %	0.985
	260.0	-0.006			
	317.3	-0.014			
	384.2	-0.063			
	384.2	-0.059			
	393.9	-0.017			
VO(acac) ₂	192.3	0.006	17955	84 %	0.972
	277.6	0.006			
	295.6	-0.021			
	374.5	-0.029			
	391.0	-0.030			
	475.4	0.022			
[VO(cat) ₂] ²⁻	186.1	-0.004	19335	65 %	0.987
	280.9	-0.017			
	366.3	-0.012			
	388.4	-0.039			
	437.4	-0.066			
[VO(dmit) ₂] ²⁻	116.8	-0.003	20120	50 %	0.999
	178.6	-0.016			
	350.7	-0.053			
	378.5	0.031			
	414.0	-0.022			
	426.6	-0.058			
Complex	Mode (cm⁻¹)	(g/Å)	(g_⊥/Å)	ES	
[V(bdt) ₃] ²⁻	351.7	-0.420	-0.357	7935	
[V(bds) ₃] ²⁻	209.8	-1.744	-0.766	6785	

^a Excited state which spin orbit coupling into the ground state.^b M(d) character in unoccupied component orbital from Loewdin population analyses.^c Loewdin metal spin density.

C. Figures

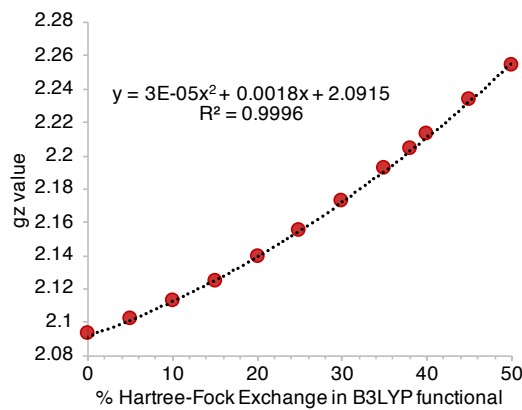


Figure S1. Hartree-Fock dependence of the calculated value of g_z for D_{4h} Cu(II)Cl₄ using the crystal structure.⁹ The experimental value is 2.221.¹⁶ Acceptable agreement between theory and experiment is obtained near the value of 38% used in the main text.

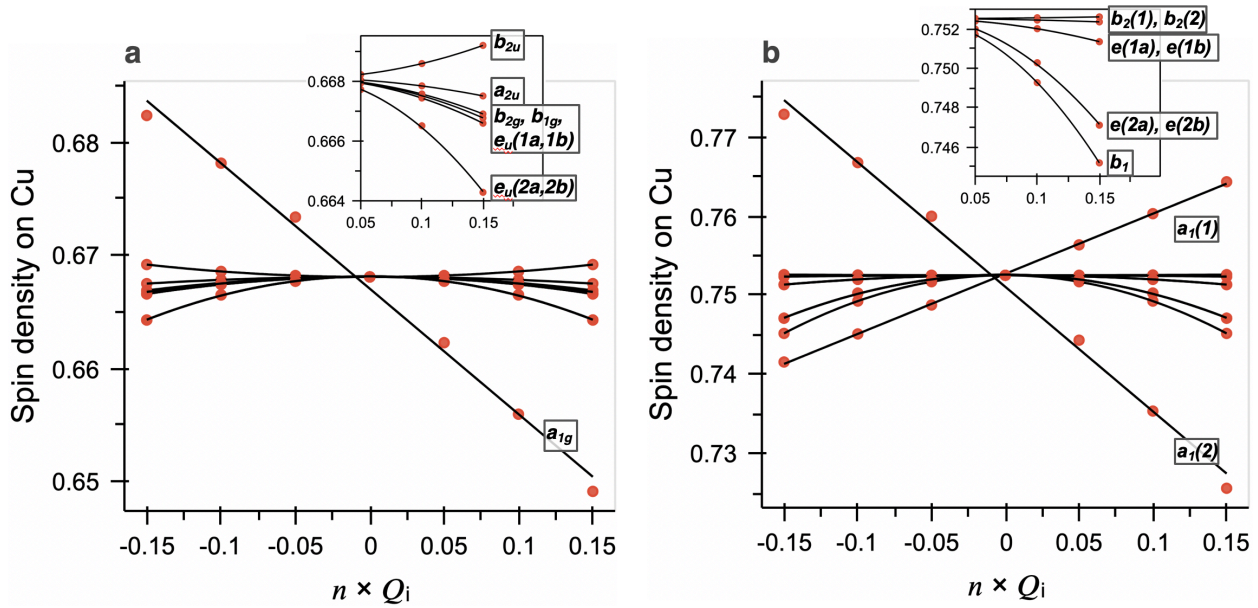


Figure S2. Spin-phonon analyses (spin density) for idealized structures of (A) D_{4h} and (B) D_{2d} $[\text{CuCl}_4]^{2-}$.

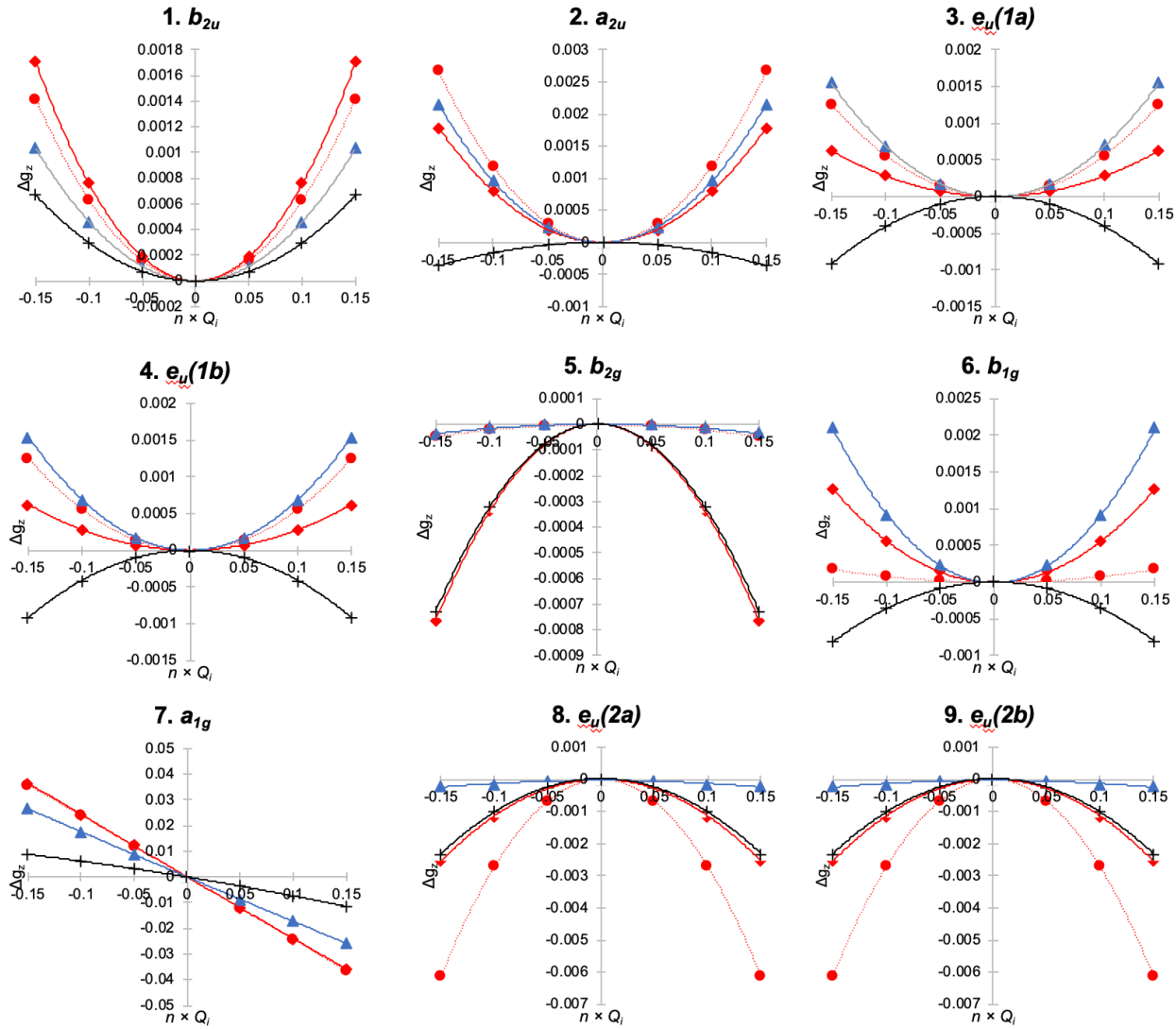


Figure S3. Spin–phonon analyses (g_z) and comparisons to equation 1 from the main text for idealized D_{4h} $[\text{CuCl}_4]^{2-}$. Blue: changes in relevant excited state energy only. Black: changes in spin density only. Solid red: changes in both spin density and excited state energy according to the LFT equation. Dotted red: DFT-computed change in g value.

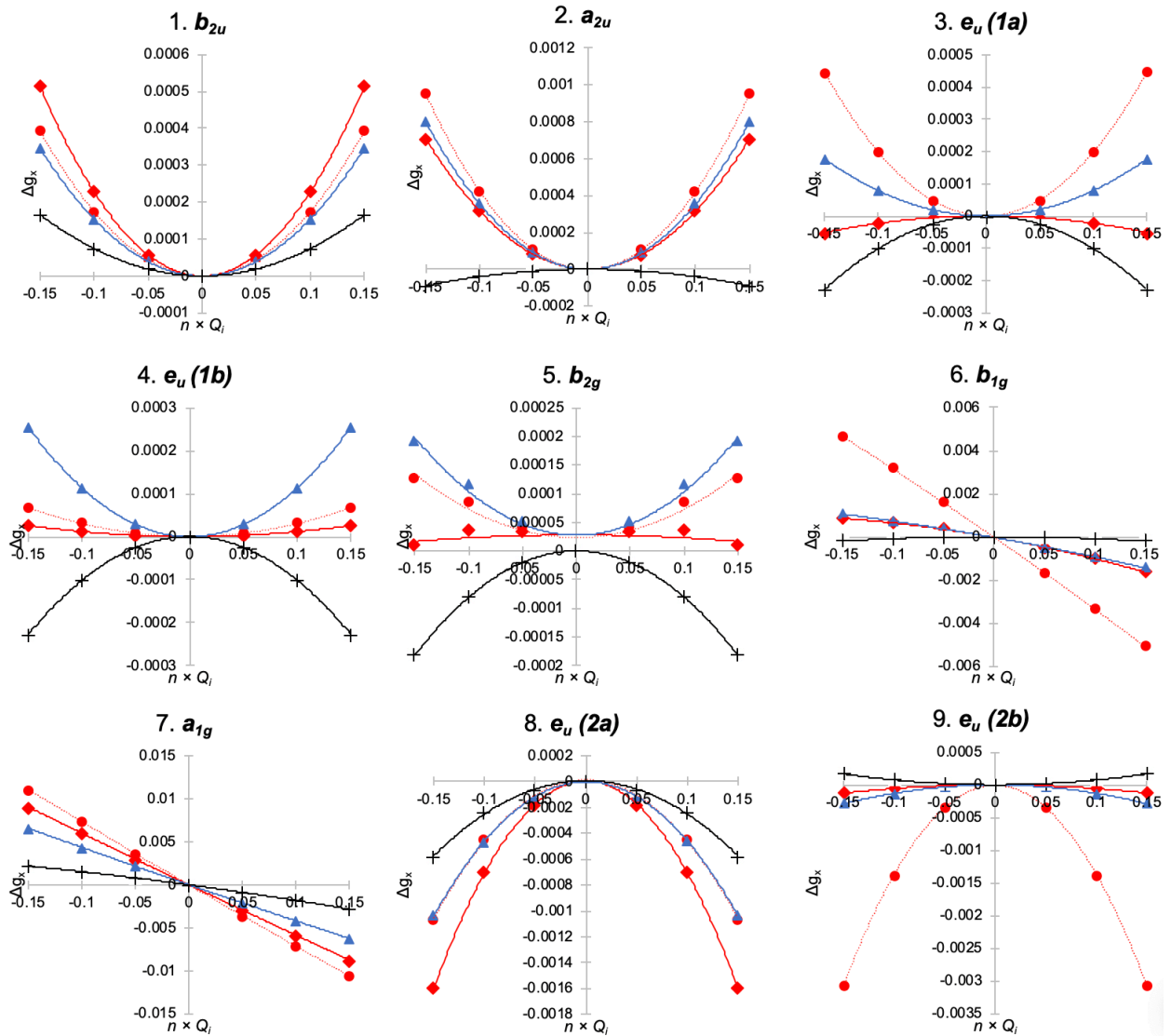


Figure S4. Spin–phonon analyses (g_x) and comparisons to equation 2 from the main text for idealized D_{4h} $[\text{CuCl}_4]^{2-}$. Blue: changes in relevant excited state energy only. Black: changes in spin density only. Solid red: changes in both spin density and excited state energy according to the LFT equation. Dotted red: DFT-computed change in g value.

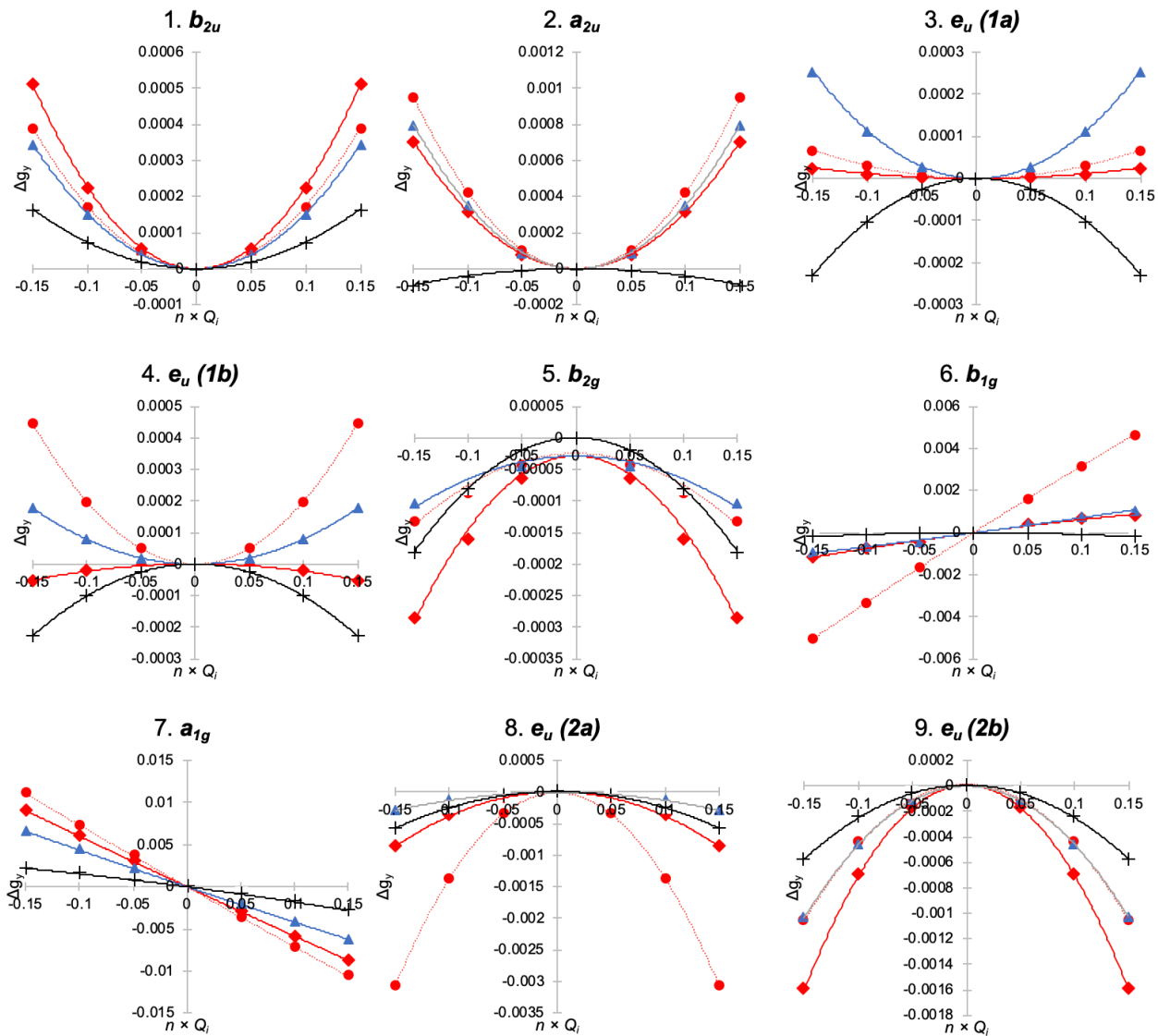


Figure S5. Spin–phonon analyses (g_y) and comparisons to equation 2 from the main text for idealized D_{4h} $[\text{CuCl}_4]^{2-}$. Blue: changes in relevant excited state energy only. Black: changes in spin density only. Solid red: changes in both spin density and excited state energy according to the LFT equation. Dotted red: DFT-computed change in g value.

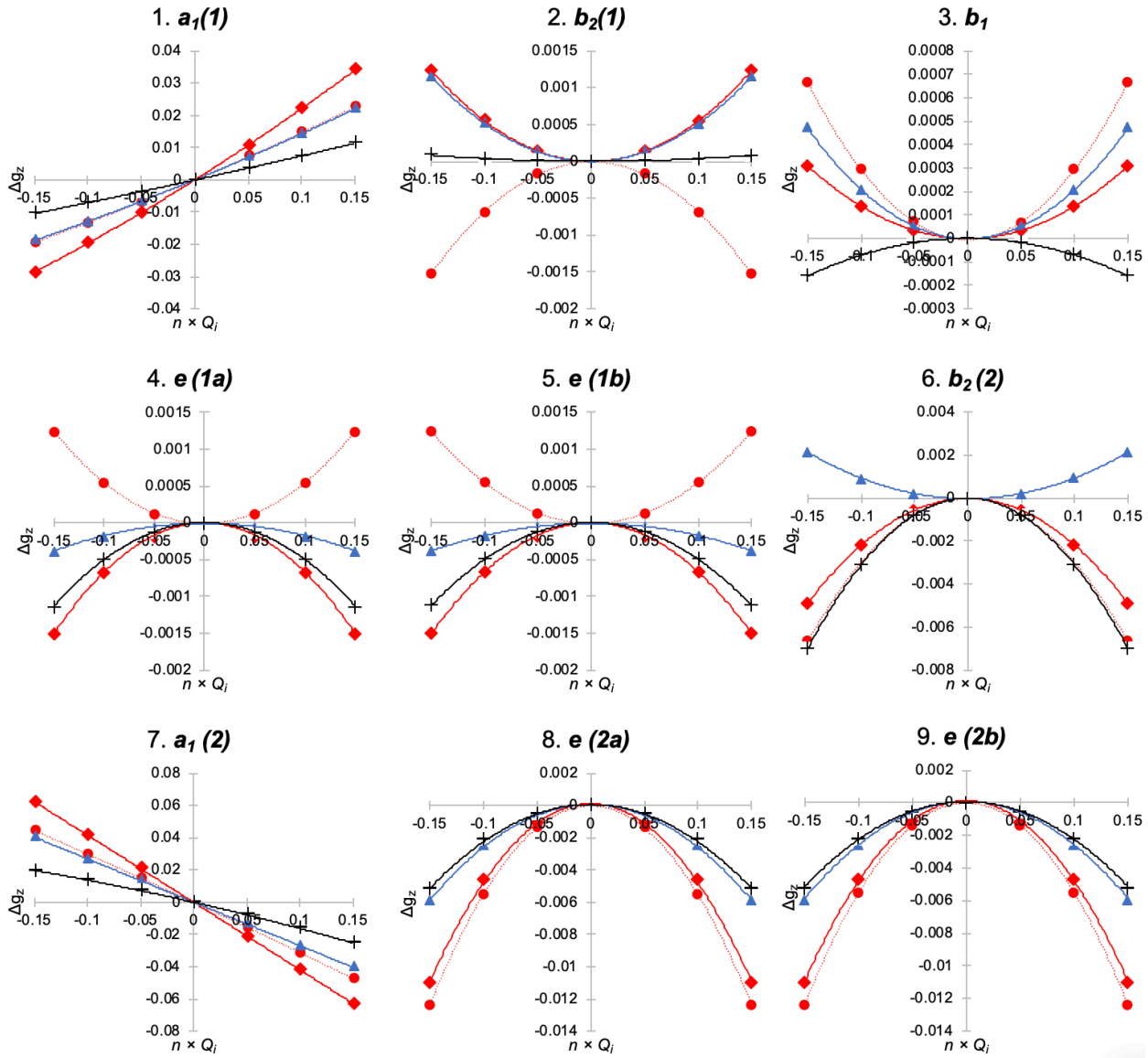


Figure S6. Spin–phonon analyses (g_z) and comparisons to equation 2 from the main text for idealized D_{2d} $[\text{CuCl}_4]^{2-}$. Blue: changes in relevant excited state energy only. Black: changes in spin density only. Solid red: changes in both spin density and excited state energy according to the LFT equation. Dotted red: DFT-computed change in g value.

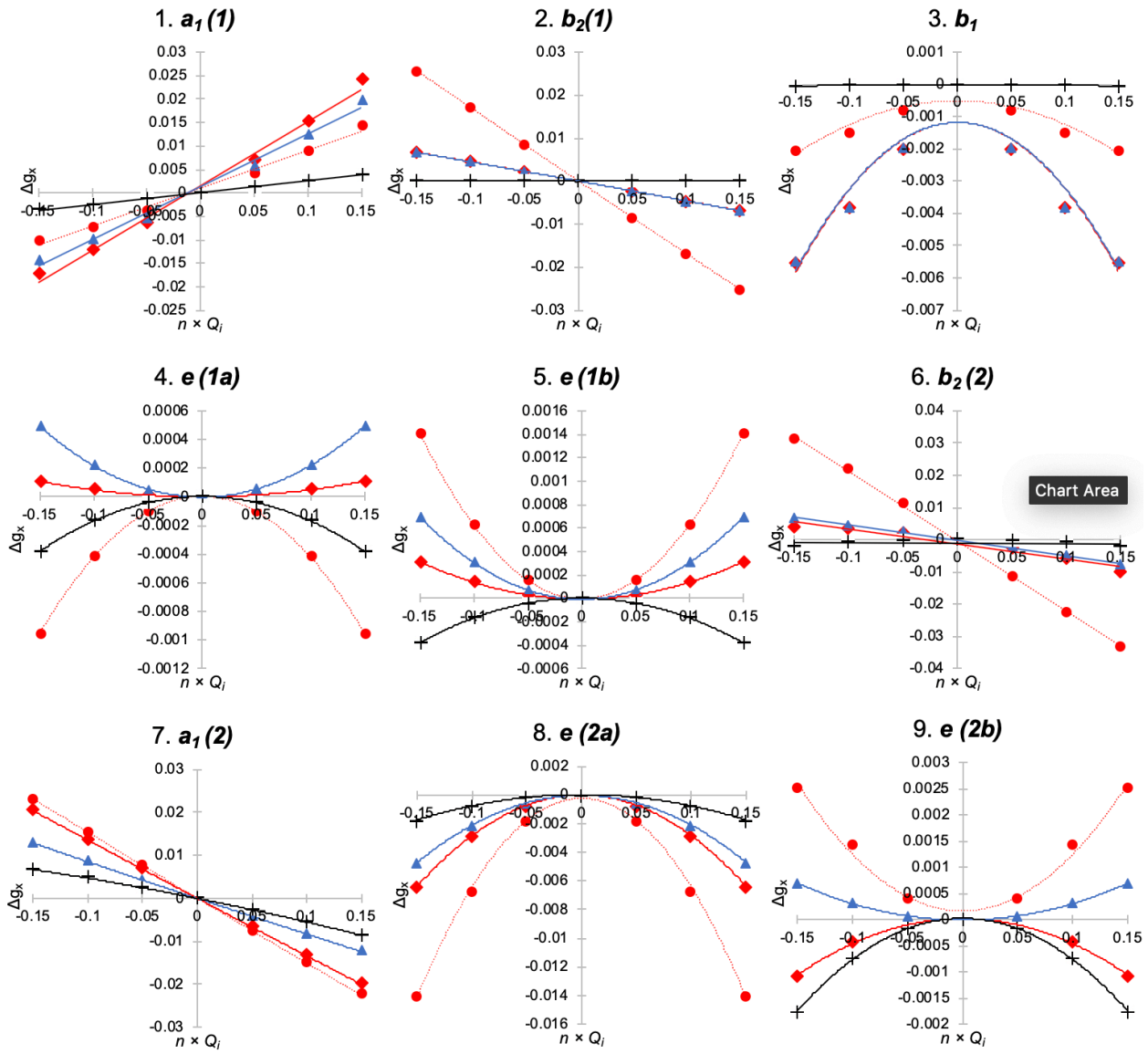


Figure S7. Spin-phonon analyses (g_x) and comparisons to equation 2 from the main text for idealized D_{2d} $[\text{CuCl}_4]^{2-}$. Blue: changes in relevant excited state energy only. Black: changes in spin density only. Solid red: changes in both spin density and excited state energy according to the LFT equation. Dotted red: DFT-computed change in g value.

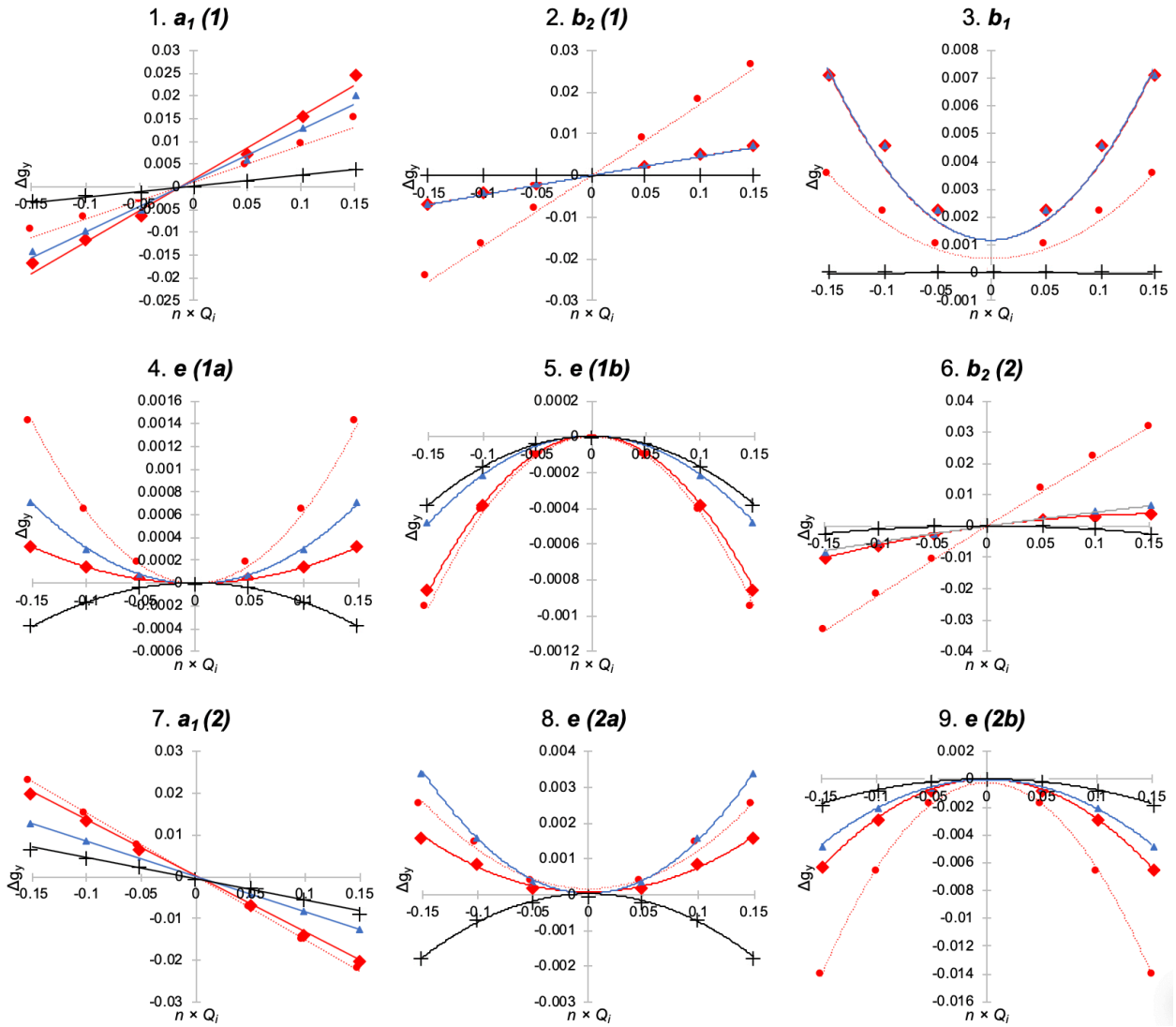


Figure S8. Spin–phonon analyses (g_y) and comparisons to equation 2 from the main text for idealized D_{2d} $[\text{CuCl}_4]^{2-}$. Blue: changes in relevant excited state energy only. Black: changes in spin density only. Solid red: changes in both spin density and excited state energy according to the LFT equation. Dotted red: DFT-computed change in g value.

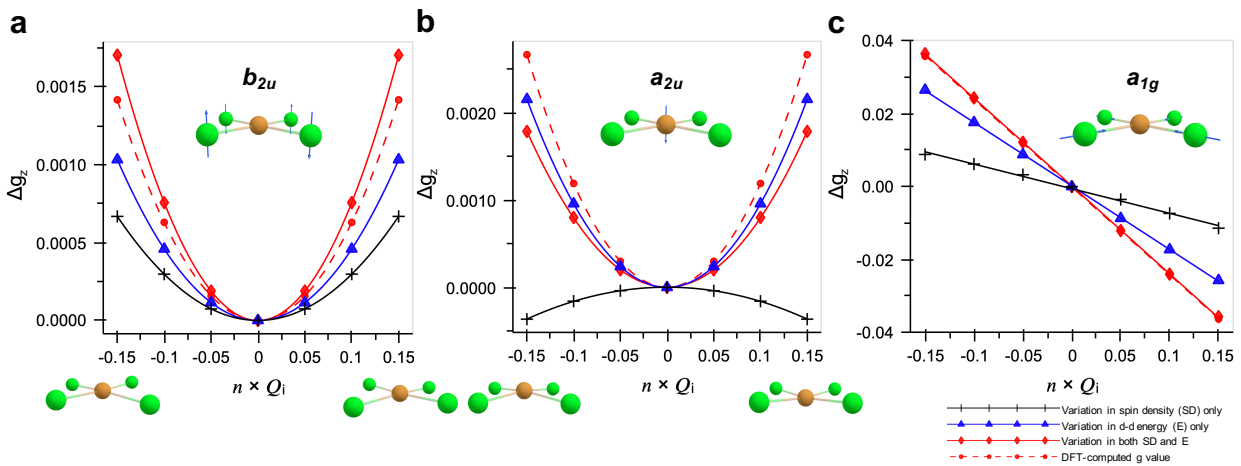


Figure S9. Independent contributions from d-d transition energy and ligand–metal covalency to the change in g_z for D_{4h} $[\text{CuCl}_4]^{2-}$. Comparisons are made between the Δg_z as calculated from the LFT expression and as computed using ORCA for modes (a) b_{2u} , (b) a_{2u} , and (c) a_{1g} . For these plots, the square of the spin density on Cu was used as a proxy for the covalency. Vector displacements are provided for each vibrational distortion.

The individual contributions to the g_z value from the $^2\text{B}_{1g}$ energy and Cu spin density can be estimated using equation 2 in combination with the DFT and TDDFT calculations. For example, for D_{4h} $[\text{CuCl}_4]^{2-}$, using the calculated Cu spin density of 0.668 and the $^2\text{B}_{1g}$ energy of 14475 cm^{-1} , equation 2 predicts a g_z value of 2.205. This is similar to the DFT calculated g_z value (2.204). For each mode, the relative change in spin density and/or $^2\text{B}_{1g}$ energy can be used to estimate a change in g_z value. The g_z value estimated from equation 2 can thus be compared directly to the DFT calculated change in g_z value along each vibrational coordinate. These plots for all normal modes and each g value are given in Figures S3-S5; the results for the b_{2u} , a_{2u} , and a_{1g} modes are given in Figures S9 (a-c), respectively. From these comparisons for the b_{2u} mode (Figure S9a), the Cu spin density and $^2\text{B}_{2g}$ energy both contribute appreciably to the change in g_z value. Furthermore, for the a_{2u} mode (Figure S9b), the change in g_z value is largely due to the change in the $^2\text{B}_{2g}$ energy; as mentioned above, a small component from the Cu spin density component actually opposes the change in g_z value determined by the $^2\text{B}_{2g}$ energy alone. Lastly, for the a_{1g} mode, the change in the g_z value is largely due to the change in $^2\text{B}_{2g}$ energy, but the spin density component contributes to a small extent. This analysis (Figure S9 and Figures S3-S5) provides a means to qualitatively decompose the

spin–phonon coupling term contributions from ground state covalency and orbital angular momentum from excited state SOC.

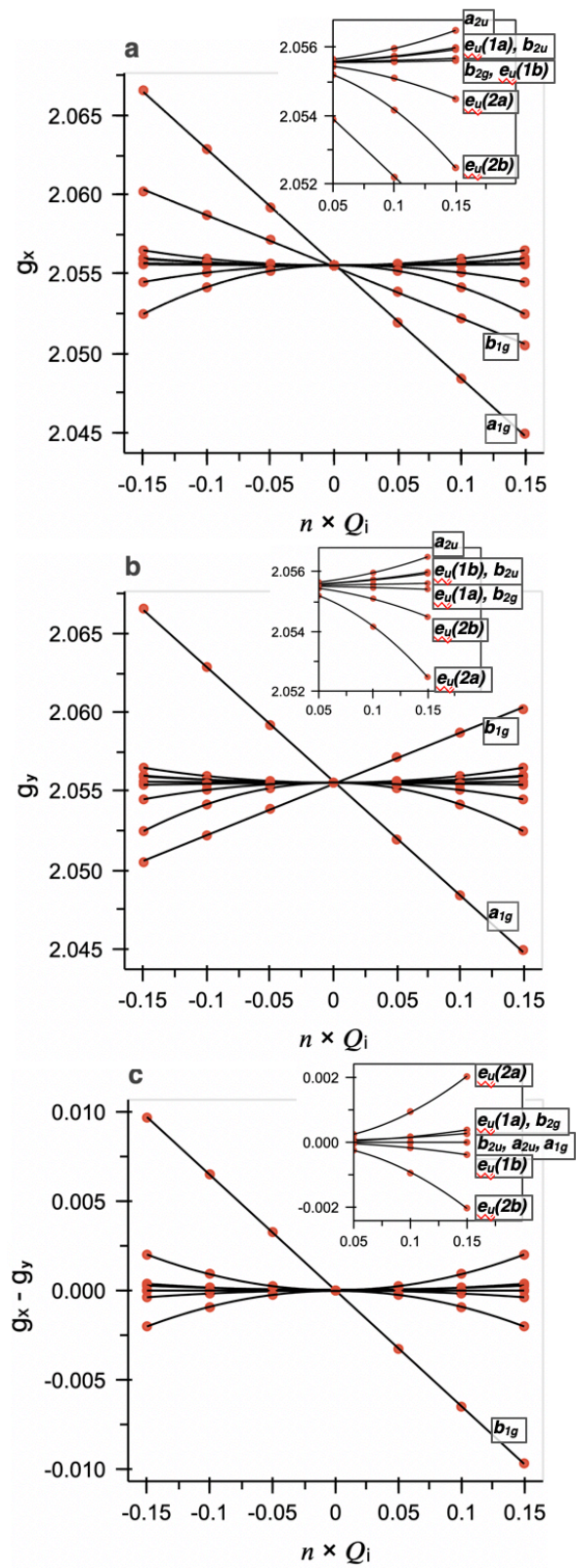


Figure S10. Spin-phonon analyses (g_x , g_y , and $g_x - g_y$) for idealized D_{4h} $[\text{CuCl}_4]^{2-}$.

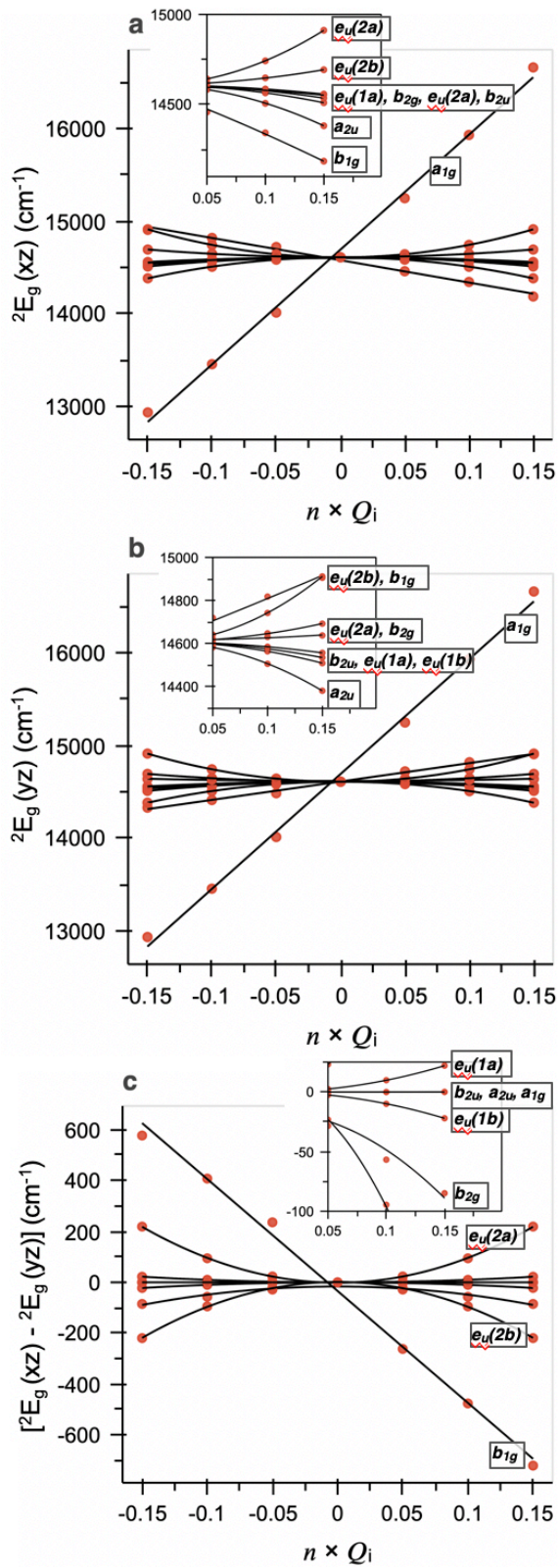


Figure S11. Spin-phonon analyses (2E_g) for idealized D_{4h} $[\text{CuCl}_4]^{2-}$.

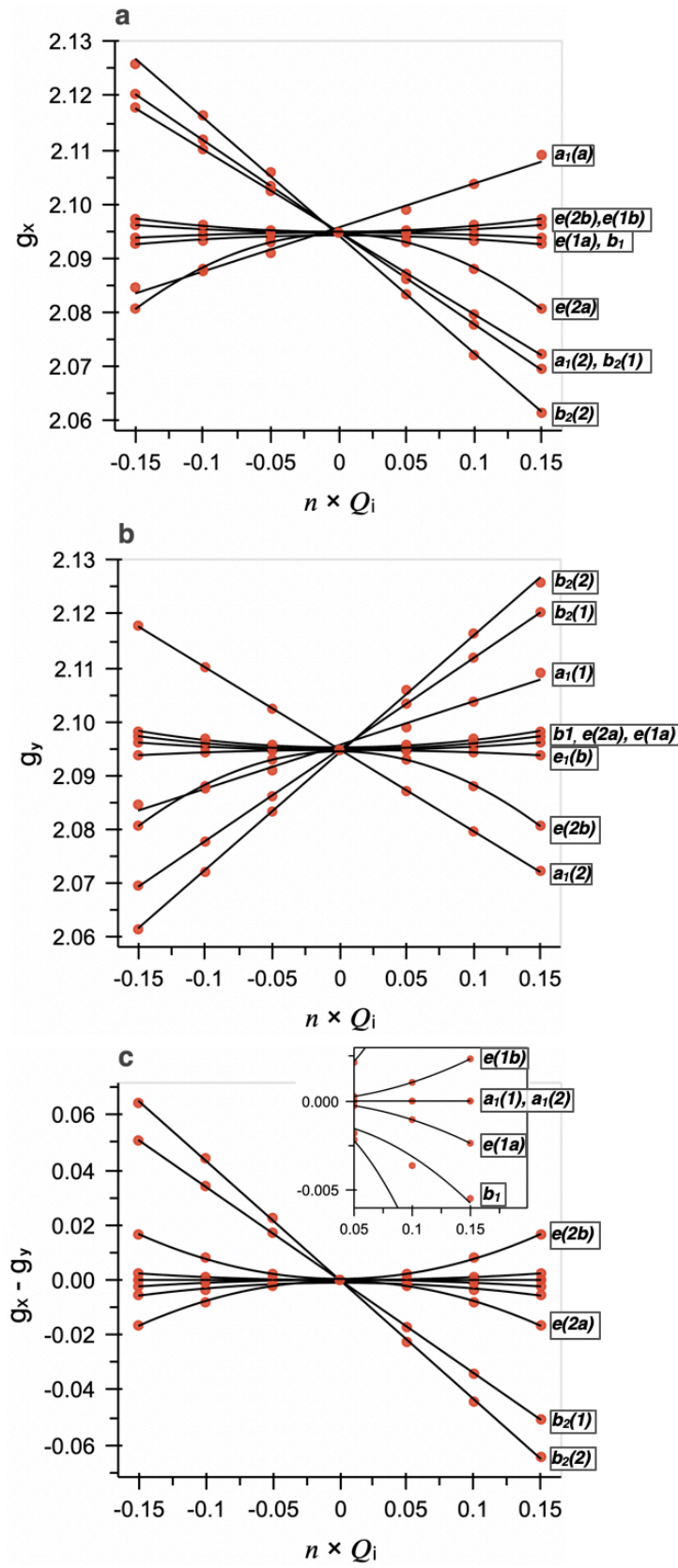


Figure S12. Spin-phonon analyses (g_x , g_y , and $g_x - g_y$) and for idealized D_{2d} $[\text{CuCl}_4]^{2-}$.

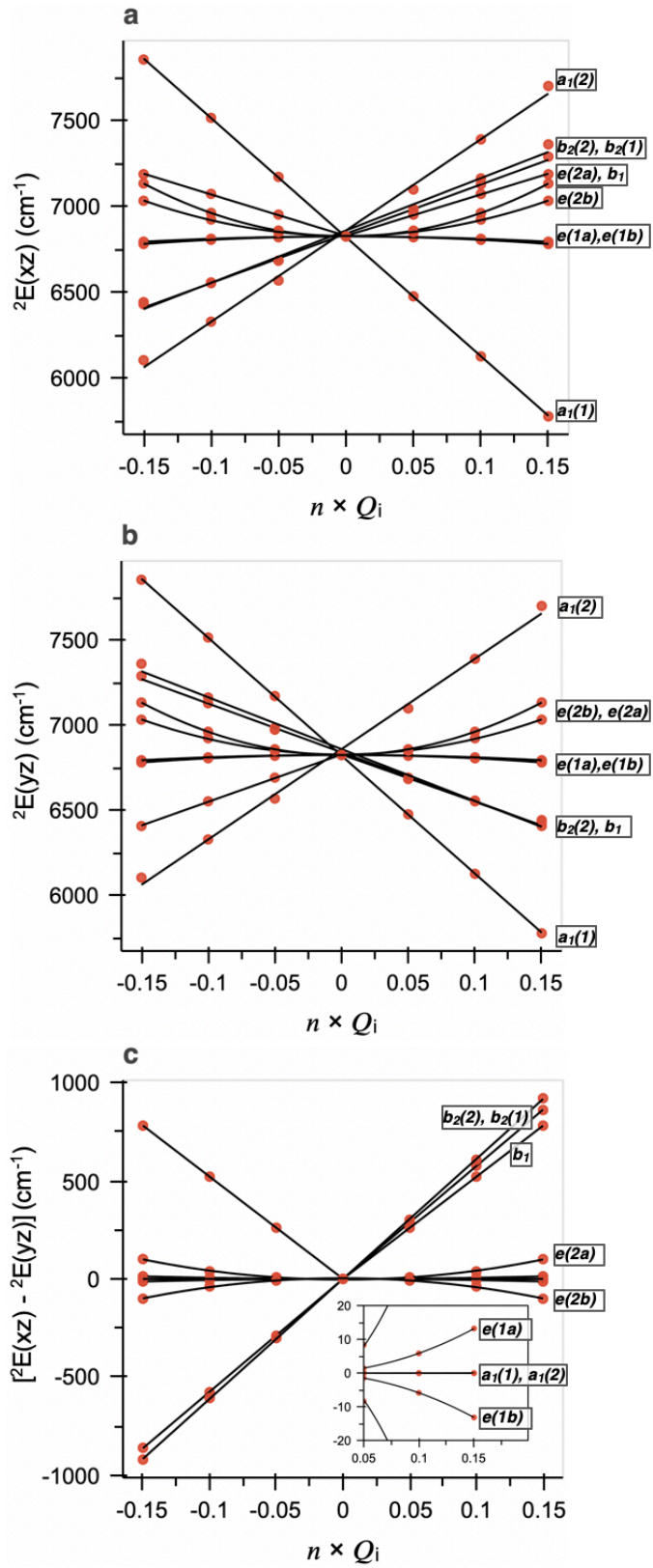


Figure S13. Spin-phonon analyses (2E) for idealized D_{2d} $[\text{CuCl}_4]^{2-}$.

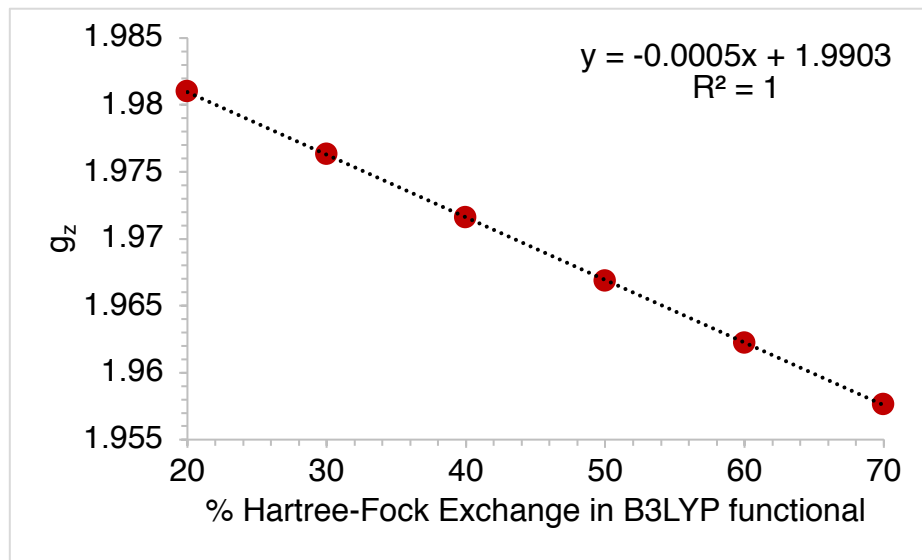


Figure S14. Hartree-Fock dependence of the calculated value of g_z for C_{4v} $[\text{VOCl}_4]^{2-}$ using the crystal structure Experimental value is 1.948. Better agreement between theory and experiment is obtained using values >50%. 60% has been used here, as it provides acceptable agreement for $[\text{VOCl}_4]^{2-}$ and the other V(IV) complexes considered here.

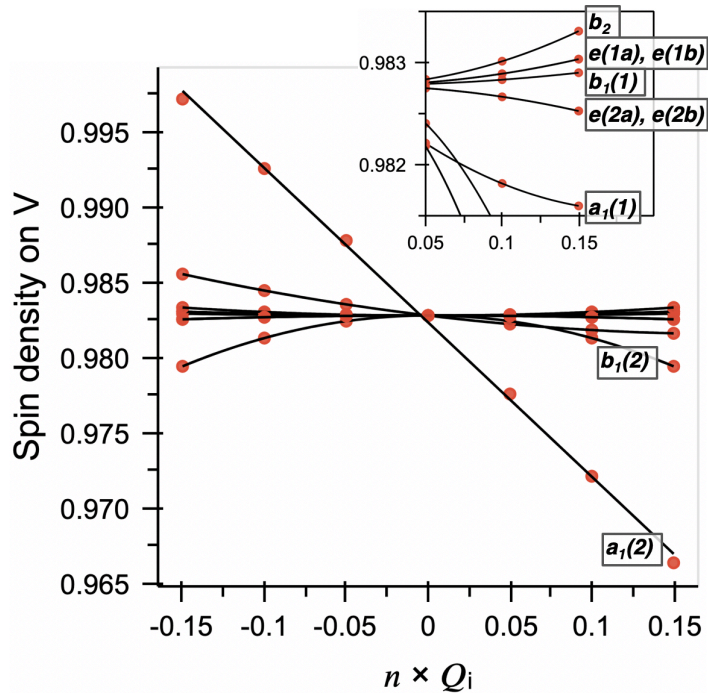


Figure S15. Spin-phonon analyses (spin density) for the idealized structure of C_{4v} $[\text{VOCl}_4]^{2-}$. The first 9 out of 12 modes are displayed.

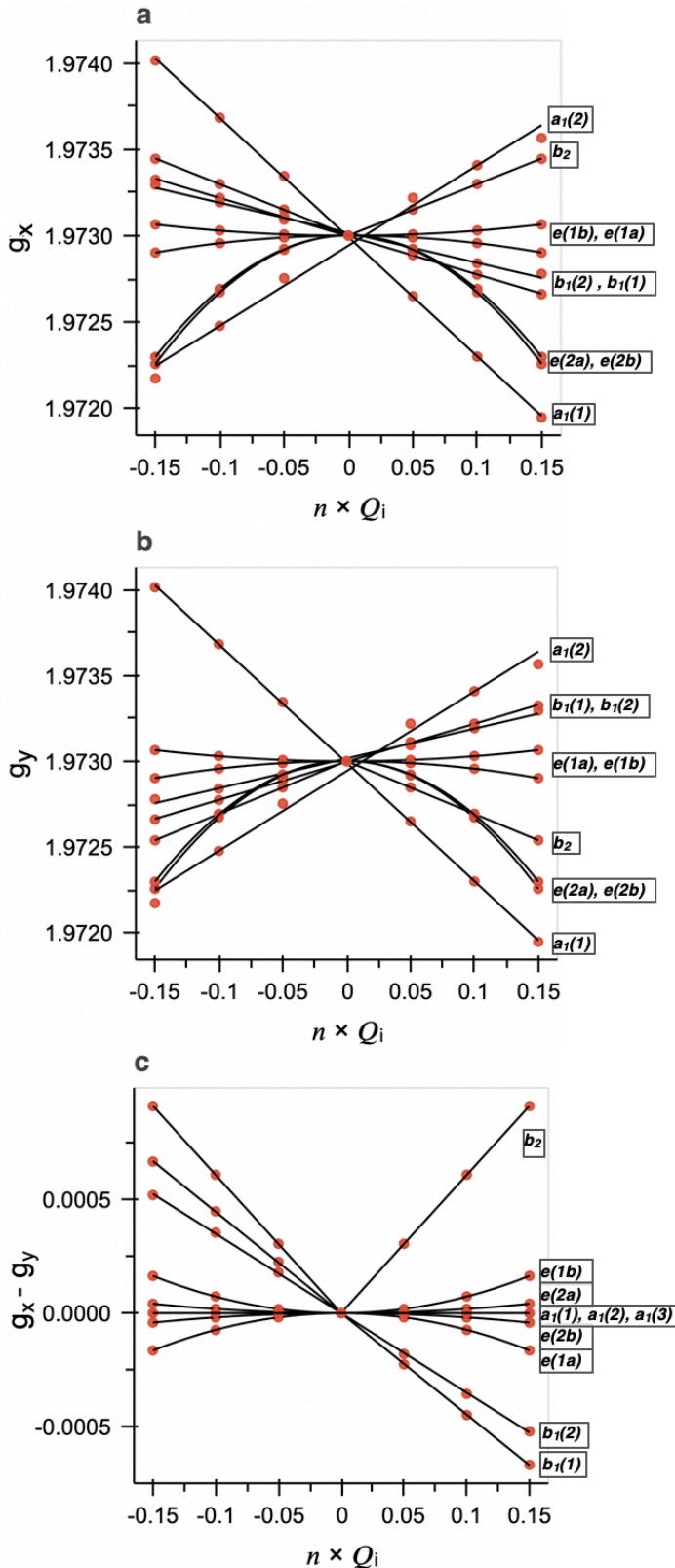


Figure S16. Spin-phonon analyses, a) g_x b) g_y , c) $g_x - g_y$ for idealized C_{4v} $[VOCl_4]^{2-}$. The first 9 out of 12 modes are displayed.

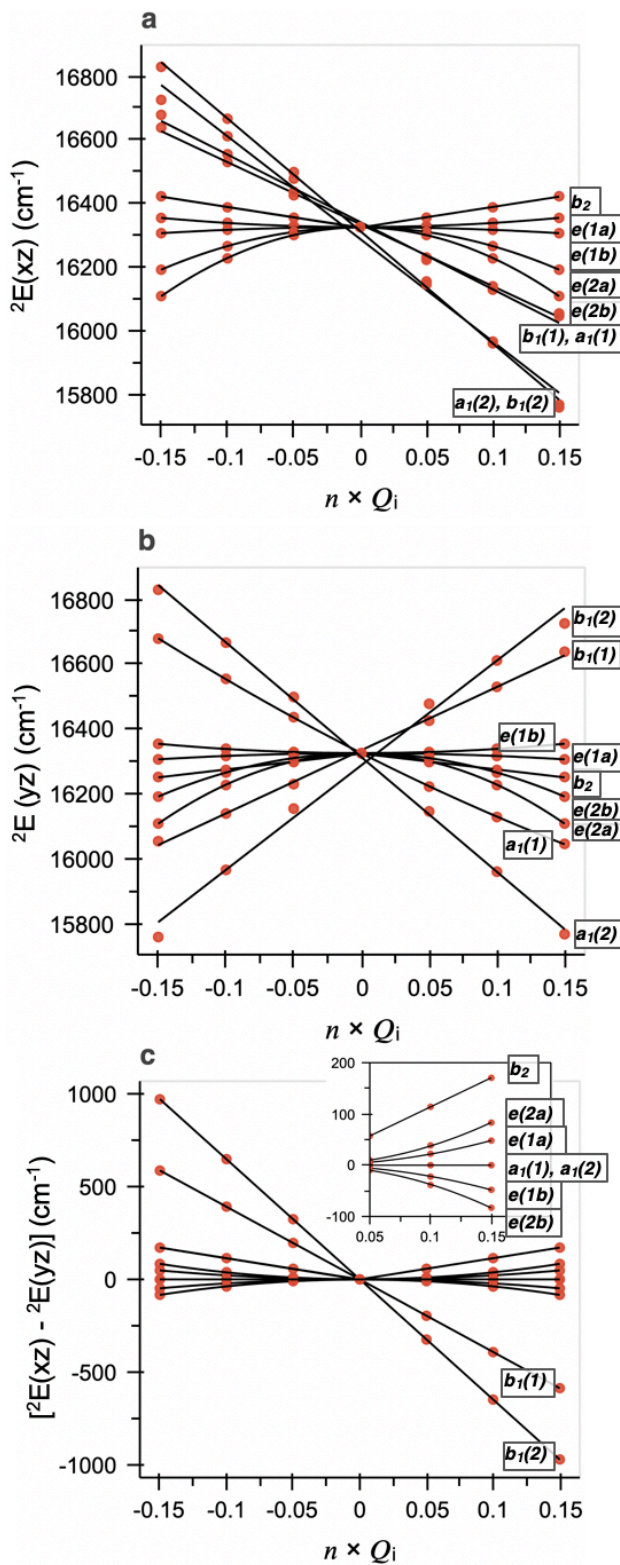


Figure S17. Spin-phonon analyses for idealized C_{4v} $[\text{VOCl}_4]^{2-}$. a) ${}^2\text{E}(\text{xz})$, b) ${}^2\text{E}(\text{yz})$, c) $[{}^2\text{E}(\text{xz}) - {}^2\text{E}(\text{yz})]$. The first 9 out of 12 modes are displayed.

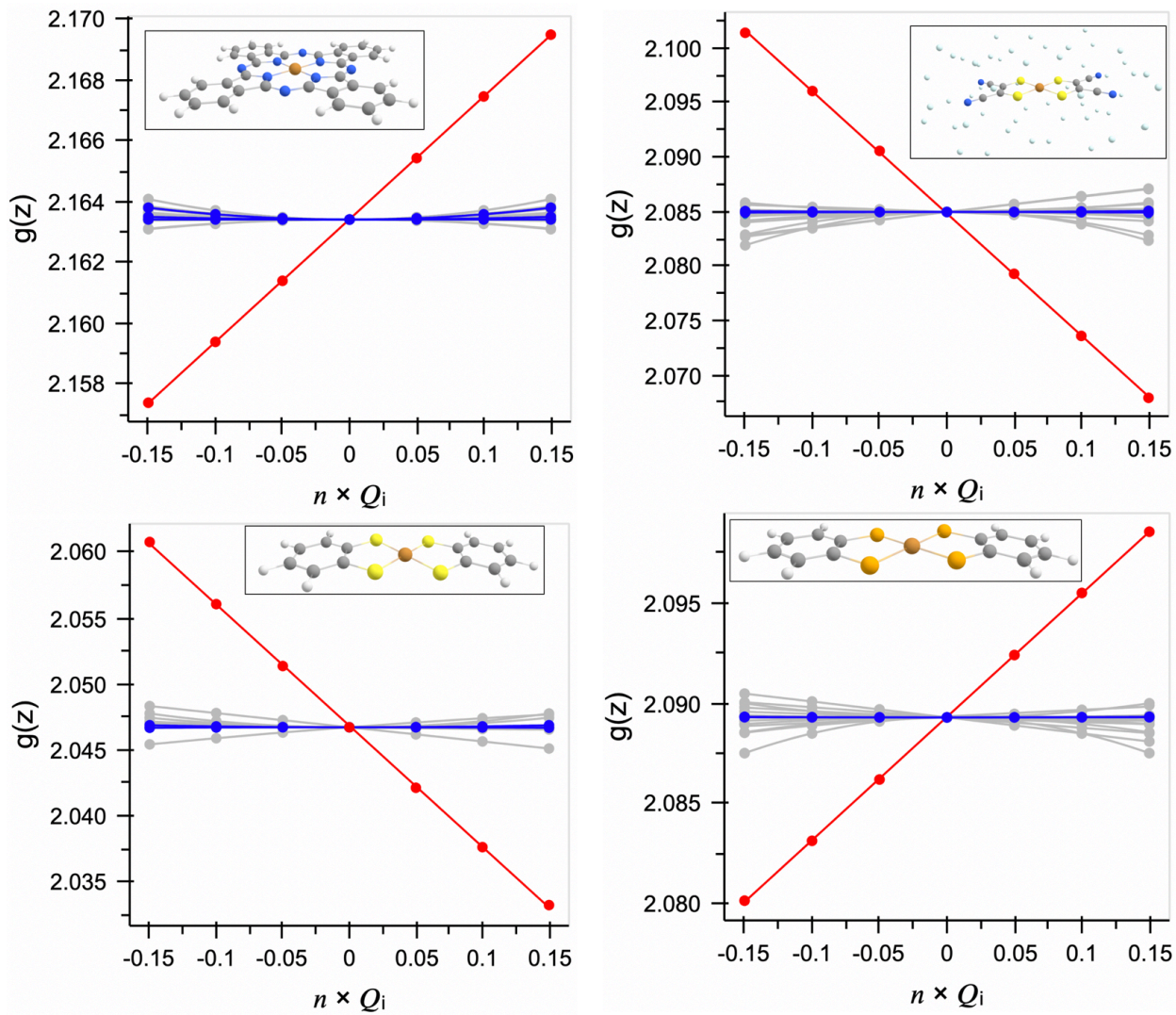


Figure S18. Spin–phonon analyses (g_z) for Cu(II) qubits. (top left) CuPc, (top right) $[\text{Cu}(\text{mnt})_2]^{2-}$, (bottom left) $[\text{Cu}(\text{bdt})_2]^{2-}$, and (bottom right) $[\text{Cu}(\text{bds})_2]^{2-}$. Red: vibrational mode with substantial M-L stretching character. Blue: vibrational mode with substantial dihedral bending character (large change in α).

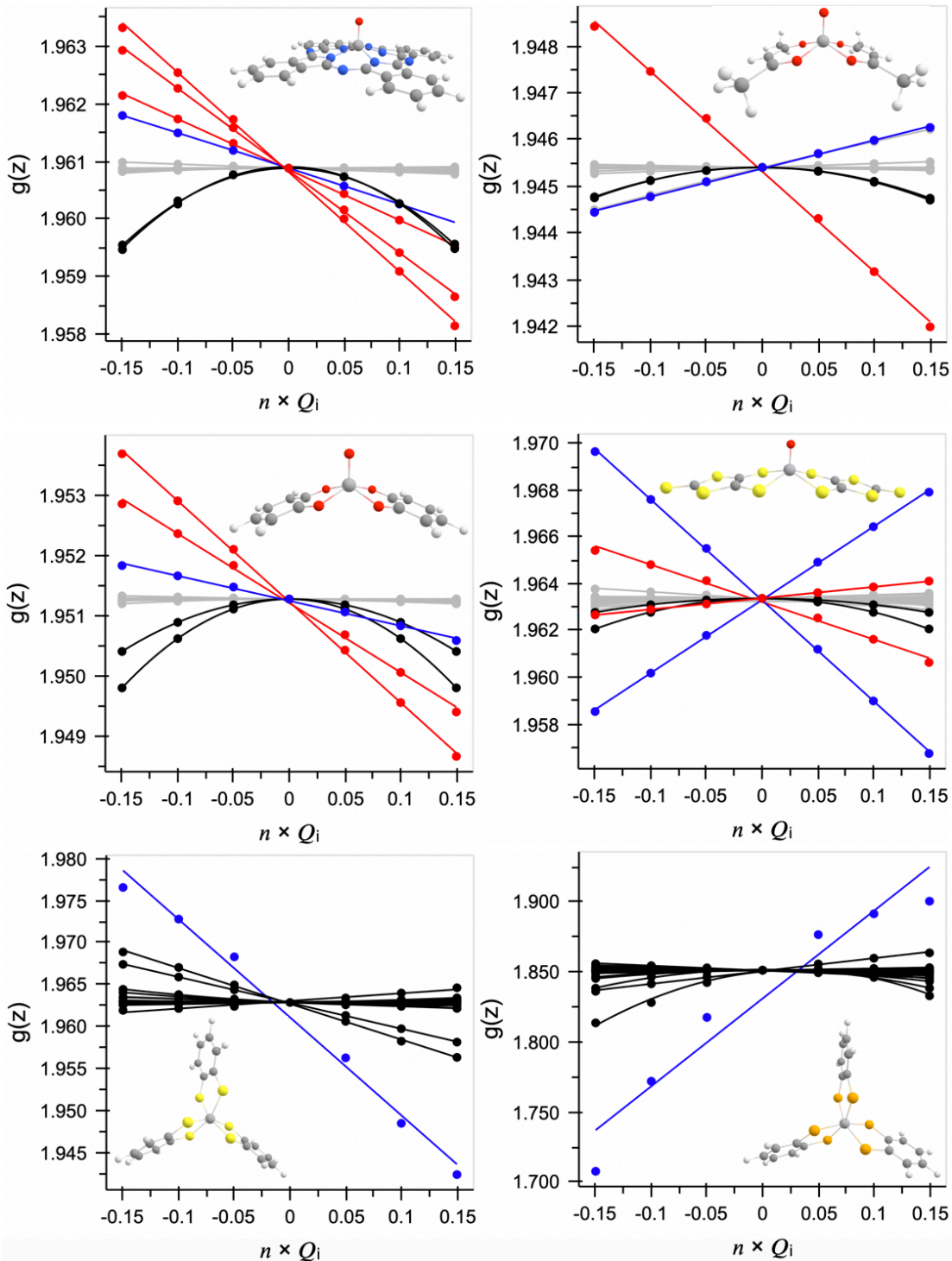


Figure S19. Spin-phonon analyses (g_z) for V(IV) qubits. (A) VOPc, (B) VO(acac)₂, (C) [VO(cat)₂]²⁻, (D) [VO(dmit)₂]²⁻, (E) [V(bdt)₃]²⁻, and (F) [V(bds)₃]²⁻. Red: vibrational mode with substantial pyramidal bending character. Blue: vibrational mode with substantial M-L stretching character (excluding M-oxo stretch). Note, due to nonlinearity of the blue slopes for [V(bdt)₃]²⁻ and [V(bds)₃]²⁻ (totally symmetric stretches), only the first two data +/- 0.05 points were used to obtain slopes.

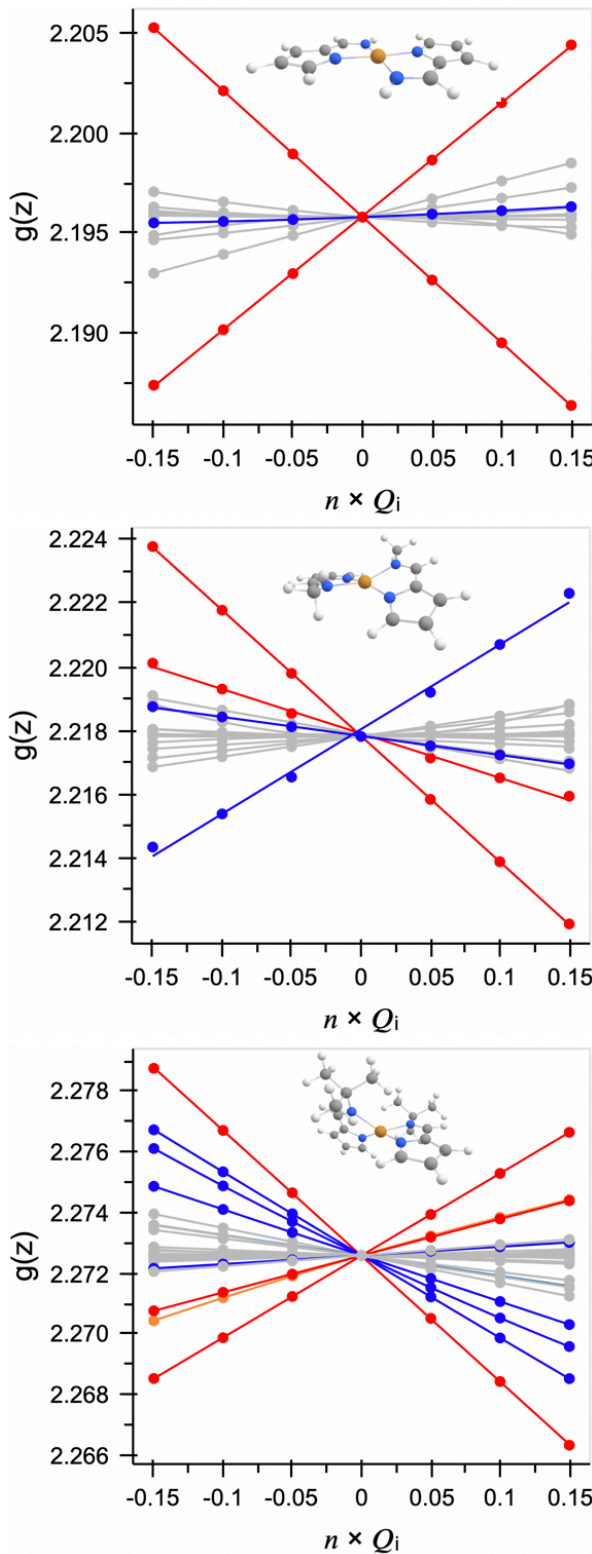


Figure S20. DFT-optimized CuN₄ complexes (R = H (top), R = Me (middle), R = *tert*-Bu (bottom)). Red: vibrational modes with substantial M-L stretching character. Blue: vibrational mode with substantial dihedral bending character (large change in α).

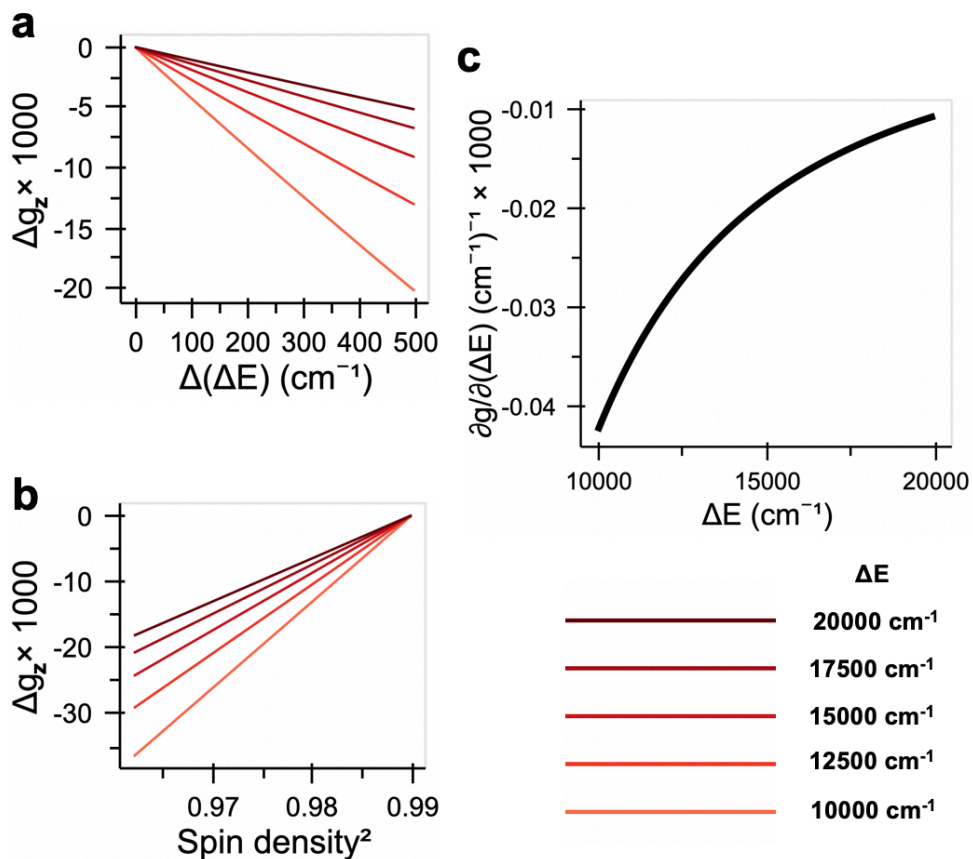


Figure S21. LFT calculations utilizing expressions from Section 2.1 in the manuscript text. (A) Variation in the g_z value as a function of ${}^2\text{B}_{2g}$ energy, (B) Variation in the g_z value as a function of spin density squared, and (C) Inverse pseudo-quadratic dependence of spin-phonon coupling term on the initial ${}^2\text{B}_{2g}$ excited state energy.

The behavior predicted in Section 2.1 and analyzed above can further be demonstrated using a series of LFT calculations. These are presented in Figure S20 for a range of initial ${}^2\text{B}_{2g}$ energies ($\Delta E = 10000 - 20000 \text{ cm}^{-1}$) and a set value of covalency (80 % Cu(d) character). The slopes of the lines in Figure S20A (i.e., the gradient in g_z value) increase with decreasing energy of the initial ${}^2\text{B}_{2g}$ excited state. Thus, for a given value of covalency, the LFT prediction indicates spin-phonon coupling terms for the g_z value are smallest for complexes that have higher energy ligand field excited states energies. This is observed for both the LFT expressions and the DFT/TDDFT data in Figures 6A and 6B. Even though the excited state coupling term of the ${}^2\text{B}_{2g}$ state (in D_{4h}) is larger than the ${}^2\text{B}_1$ state (in D_{2d}) (also compare blue lines in Figure 4A), the resultant effect on the gradient in g_z value is smaller because the initial energy

of ${}^2\text{B}_{2g}$ state is higher in energy than the ${}^2\text{B}_1$ state. Lastly, the slopes of the g_z value vs. ${}^2\text{B}_{2g}$ energy shown in Figure S20A exhibit an inverse pseudo-quadratic dependence on the initial energy of the ${}^2\text{B}_{2g}$ excited state (Figure S20C).

The covalency contributions to the spin–phonon coupling terms can also be evaluated. For a given ${}^2\text{B}_{2g}$ energy (e.g., 10000 cm^{-1}), the gradient in the g_z value for a change in covalency can be calculated for a series of initial covalency values (Figure S20B). The slopes of these lines increase with decreasing covalency. Thus, the spin–phonon coupling term for the g_z value is smaller for more covalent ligand–metal bonds, and this coupling term is linearly dependent on the covalency of a given ligand–metal bond. Again, this behavior predicted by LFT and is also observed for DFT calculations presented in Figures 6A and 6C.

D. DFT Structures and Input Coordinates

[CuCl₄]²⁻ crystal structure

```
Cl -0.002786 -2.280699  0.000000
Cl -2.247278 -0.003002  0.000000
Cu  0.000000  0.000000  0.000000
Cl  0.002786  2.280699  0.000000
Cl  2.247278  0.003002  0.000000
```

[CuCl₄]²⁻ idealized structure

```
Cl  0.000000 -2.264000  0.000000
Cl -2.264000  0.000000  0.000000
Cu  0.000000  0.000000  0.000000
Cl  0.000000  2.264000  0.000000
Cl  2.264000  0.000000  0.000000
```

[Cu(mnt)₂]²⁻ crystal structure He cage¹⁷

Cu	0.001242	0.000571	0.000099
N	5.350804	-1.883487	0.221212
N	-5.346332	1.888441	-0.221762
N	5.258176	2.173372	-0.015008
N	-5.255549	-2.172419	0.015367
S	1.692644	-1.584810	0.034526
S	-1.689934	1.586102	-0.033510
S	1.619168	1.690587	-0.126304
S	-1.617007	-1.689183	0.125983
C	3.122068	-0.596224	0.082898
C	-3.119663	0.597899	-0.081575
C	4.359048	-1.288467	0.163586
C	-4.356045	1.291124	-0.162608
C	3.091239	0.778285	0.020976
C	-3.089067	-0.776603	-0.020200
C	4.295102	1.531016	0.014252
C	-4.292806	-1.529546	-0.013695
He	6.188799	-0.937495	-3.096306
He	-6.189224	0.938056	3.096285
He	7.719578	-2.226888	-1.917291
He	-7.719989	2.227491	1.917301
He	2.268341	5.208778	1.258576
He	-2.268754	-5.208190	-1.258570
He	0.832704	-3.221674	-2.847842
He	-0.833106	3.222253	2.847850
He	1.378397	2.593504	2.995096
He	-1.378809	-2.592926	-2.995089
He	5.519905	2.227175	3.165540
He	-5.520312	-2.226597	-3.165555
He	6.773620	3.621984	1.838571
He	-0.528791	-1.914067	3.874611
He	0.528378	1.914655	-3.874611
He	-6.774018	-3.621400	-1.838565
He	6.330228	5.869329	1.772994
He	5.903450	-3.601739	-4.093076
He	0.734151	-3.465172	2.756368
He	-0.734562	3.465750	-2.756372
He	-5.903862	3.602317	4.093084
He	-6.330644	-5.868751	-1.772984
He	4.172094	-2.725347	-2.872268
He	-4.172504	2.725921	2.872274
He	2.887551	-4.099351	-1.539883
He	-2.887955	4.099942	1.539884
He	4.643875	-4.899196	0.435124
He	-4.644286	4.899720	-0.435148
He	6.908665	-1.219852	2.567387
He	5.446667	-4.587814	2.571021

He	-5.447067	4.588413	-2.571031
He	-6.909076	1.220433	-2.567391
He	7.587035	0.143413	0.860741
He	-7.587428	-0.142837	-0.860738
He	1.980676	-0.562458	-3.210510
He	-1.981065	0.563019	3.210511
He	3.816109	0.691256	-2.609753
He	-3.816476	-0.690641	2.609766
He	3.603320	3.115971	-3.882709
He	-3.603739	-3.115394	3.882705
He	6.904520	-4.226074	-0.563357
He	-6.904959	4.226712	0.563409
He	3.956188	6.048382	-1.228601
He	8.137040	-3.106397	0.983741
He	4.218233	-2.701279	4.154707
He	-4.218646	2.701867	-4.154700
He	-8.137470	3.106985	-0.983726
He	-3.956599	-6.047805	1.228598
He	6.134159	5.471991	-0.864728
He	2.650999	-1.606071	2.908682
He	-2.651410	1.606648	-2.908686
He	-6.134570	-5.471404	0.864734
He	7.054786	3.662271	-1.970599
He	2.245377	0.641117	3.270731
He	-2.245780	-0.640530	-3.270723
He	-7.055198	-3.661694	1.970606

CuPc optimized structure

Cu	1.929292	-0.000001	-0.000075
C	-0.816622	-1.133209	-0.047251
C	2.662694	-4.145743	-0.018180
C	3.389802	-5.327906	-0.015873
C	2.683996	-6.517341	-0.034066
C	1.284308	-6.528964	-0.054295
C	0.558518	-5.351405	-0.056627
C	1.265695	-4.157327	-0.038326
C	0.842295	-2.765786	-0.034679
C	-2.214832	-0.732876	-0.065020
C	-3.396860	-1.459978	-0.087676
C	-4.586241	-0.753945	-0.100581
C	-4.598029	0.645896	-0.091101
C	-3.420701	1.371474	-0.068500
C	-2.226580	0.664090	-0.055594
C	-0.835472	1.087821	-0.032306
C	3.062952	-2.747521	-0.002689
H	4.464599	-5.313798	-0.000407
H	3.216475	-7.452508	-0.032793
H	0.767555	-7.472814	-0.068156
H	-3.382884	-2.534854	-0.094865
H	-5.521234	-1.286444	-0.118247
H	-5.541833	1.162810	-0.101667
H	-3.424706	2.446437	-0.061215
N	-0.418924	-2.388251	-0.050220
N	-0.038656	-0.016058	-0.028118
N	-0.459287	2.349516	-0.018312
N	1.912461	1.969569	0.013234
N	3.897240	0.016061	0.028031
N	1.946125	-1.969570	-0.013321
N	4.317871	-2.349515	0.018258
C	0.795633	2.747519	0.002627
C	3.016288	2.765787	0.034621
C	4.675206	1.133213	0.047201
C	4.694055	-1.087818	0.032248
C	1.195887	4.145741	0.018147
C	2.592885	4.157328	0.038294
N	4.277508	2.388255	0.050174
C	6.073418	0.732880	0.065005
C	6.085164	-0.664086	0.055576
C	0.468774	5.327899	0.015871
C	3.300058	5.351407	0.056633
C	7.255446	1.459980	0.087706
C	7.279283	-1.371472	0.068524
C	1.174577	6.517336	0.034100
H	-0.606022	5.313787	0.000404
C	2.574264	6.528963	0.054331

C	8.444826	0.753944	0.100654
H	7.241471	2.534856	0.094898
C	8.456612	-0.645896	0.091172
H	7.283287	-2.446435	0.061237
H	0.642096	7.452502	0.032852
H	3.091015	7.472814	0.068223
H	9.379819	1.286442	0.118356
H	9.400415	-1.162812	0.101771
H	-0.516354	-5.355312	-0.072228
H	4.374930	5.355317	0.072236

[Cu(bdt)₂]²⁻ crystal structure (H-optimized)

Cu	-0.246333	4.840524	0.988186
S	-0.297451	7.010976	0.973118
S	1.922436	4.810648	1.000521
C	2.367678	6.499871	1.080609
C	3.698797	6.876472	1.137466
H	4.462439	6.116629	1.147774
C	4.035157	8.205599	1.189637
H	5.079044	8.487390	1.231583
C	3.061918	9.202347	1.160317
H	3.337319	10.245155	1.193239
C	1.736583	8.815746	1.112850
H	0.954494	9.558068	1.093694
C	1.378850	7.481657	1.071483
S	-0.195214	2.670072	1.003254
C	-1.871516	2.199391	0.904890
C	-2.860344	3.181176	0.895764
S	-2.415101	4.870399	0.975851
C	-4.191462	2.804575	0.838906
H	-4.955105	3.564419	0.828596
C	-4.527823	1.475448	0.786736
H	-5.571709	1.193657	0.744782
C	-3.554583	0.478701	0.816055
H	-3.829986	-0.564107	0.783138
C	-2.229249	0.865302	0.863523
H	-1.447160	0.122979	0.882678

[Cu(bds)₂]²⁻ crystal structure (H-optimized)

Se	2.413500	0.000148	-0.002234
Se	-0.002019	2.377198	0.001096
Cu	0.000006	0.000004	0.000006
C	1.828800	2.827746	0.141805
C	2.828824	1.853727	0.131995
C	2.192605	4.178527	0.280461
H	1.415755	4.924644	0.300541
C	3.518228	4.551426	0.392536
H	3.775844	5.595216	0.497960
C	4.504059	3.592788	0.359040
H	5.543168	3.877358	0.439563
C	4.168573	2.251722	0.233388
H	4.939919	1.500051	0.218160
Se	-2.413541	-0.000012	0.002216
Se	0.001902	-2.377104	-0.001162
C	-1.828840	-2.827610	-0.141824
C	-2.828865	-1.853590	-0.132013
C	-2.192722	-4.178433	-0.280528
H	-1.415864	-4.924545	-0.300632
C	-3.518268	-4.551290	-0.392554
H	-3.775907	-5.595075	-0.497978
C	-4.504100	-3.592651	-0.359058
H	-5.543201	-3.877258	-0.439582
C	-4.168690	-2.251628	-0.233454
H	-4.940029	-1.499952	-0.218244

CuN₄ (R = H) optimized structure

Cu	0.000452	0.000420	-0.032815
C	2.523472	1.222653	-0.069467
C	1.621652	2.301182	0.034792
C	1.772180	3.687526	0.114715
C	0.485159	4.209757	0.206111
C	-0.387969	3.116559	0.176993
N	2.041251	0.022674	-0.117011
N	0.288530	1.970138	0.073689
N	-2.040268	-0.017550	-0.117144
N	-0.288142	-1.972122	-0.011491
C	-2.522873	-1.218304	-0.121172
C	-1.621416	-2.300673	-0.064089
C	0.388027	-3.122140	0.041299
C	-1.772371	-3.689143	-0.044675
C	-0.485468	-4.215276	0.023130
H	3.588720	1.407793	-0.107420
H	2.696894	4.230936	0.107163
H	0.205657	5.241397	0.284455
H	-1.460023	3.133733	0.229846
H	-3.588211	-1.401245	-0.166516
H	1.460108	-3.141934	0.092722
H	-2.697282	-4.231392	-0.075393
H	-0.206268	-5.249435	0.056234
H	-2.713241	0.724694	-0.161990
H	2.714467	-0.716670	-0.194338

CuN₄ (R = Me) optimized structure

Cu	0.000095	-0.000371	-0.001644
N	0.162667	1.968189	0.178463
C	-0.537149	3.055567	0.531942
H	-1.567796	2.989866	0.820929
N	2.010380	0.172067	-0.511367
C	0.257616	4.200087	0.465966
H	-0.051485	5.200001	0.696784
C	1.520289	3.780514	0.045240
H	2.389237	4.388257	-0.115990
C	1.431118	2.399799	-0.119954
C	2.368518	1.408296	-0.493338
H	3.378397	1.698414	-0.760391
C	2.958383	-0.853529	-0.895609
H	3.872060	-0.422078	-1.298491
H	2.521105	-1.505098	-1.644424
H	3.219913	-1.469590	-0.040383
N	-0.146129	-1.942106	0.376902
C	0.576613	-2.992284	0.791386
H	1.622812	-2.902333	1.009248
C	-0.217978	-4.134925	0.885849
H	0.106967	-5.108599	1.194099
C	-1.504946	-3.753857	0.503842
H	-2.380595	-4.371377	0.455877
C	-1.429333	-2.396111	0.199622
C	-2.389890	-1.442145	-0.211096
N	-2.036446	-0.214701	-0.370462
C	-3.007899	0.771922	-0.795828
H	-3.943896	0.306704	-1.097056
H	-2.618481	1.343958	-1.631076
H	-3.217305	1.471005	0.008361
H	-3.413324	-1.753147	-0.387669

CuN₄ (R = t-Bu) optimized structure

Cu	-0.002134	-0.001526	-0.007537
N	0.232946	1.902783	0.423070
C	-0.382564	2.923503	1.041897
H	-1.383534	2.829989	1.415686
C	0.454211	4.034933	1.108857
H	0.215371	4.981625	1.550847
C	1.652660	3.665911	0.493002
H	2.531428	4.267408	0.364751
C	1.487108	2.343865	0.087837
C	2.365631	1.420057	-0.535367
H	3.336152	1.780236	-0.844029
N	2.000955	0.200508	-0.722002
C	2.881979	-0.789080	-1.383967
C	4.001032	-0.145493	-2.214721
H	4.727104	0.376376	-1.600251
H	3.603539	0.550779	-2.946784
H	4.536132	-0.921916	-2.750205
C	3.508080	-1.679463	-0.300887
H	2.742743	-2.184431	0.273148
H	4.113604	-1.087349	0.378258
H	4.143516	-2.434866	-0.753185
C	2.003355	-1.636662	-2.312581
H	1.207124	-2.119627	-1.759405
H	2.596815	-2.408226	-2.792610
H	1.559754	-1.020108	-3.088240
N	-0.305981	-1.848700	0.593032
C	0.216311	-2.791226	1.394631
H	1.160601	-2.650111	1.883369
C	-0.629772	-3.894819	1.472565
H	-0.457343	-4.785855	2.042639
C	-1.734828	-3.604035	0.668720
H	-2.593334	-4.222610	0.493187
C	-1.508496	-2.332975	0.146677
C	-2.289877	-1.489612	-0.685345
H	-3.213259	-1.888429	-1.079345
N	-1.894128	-0.295461	-0.954206
C	-2.665825	0.609167	-1.836756
C	-3.682453	-0.125984	-2.721340
H	-4.488500	-0.570220	-2.146819
H	-3.208533	-0.904812	-3.310850
H	-4.132950	0.582795	-3.407283
C	-3.406579	1.627142	-0.957518
H	-2.710198	2.196567	-0.356836
H	-4.103345	1.124769	-0.293769
H	-3.966457	2.323054	-1.574885
C	-1.659499	1.334377	-2.739443
H	-0.931180	1.877905	-2.149959

H -2.171230 2.044385 -3.381261
H -1.132557 0.626201 -3.371455

[VOCl₄]²⁻ crystal structure

V	0.000000	0.000000	0.000000
O	0.000000	0.000000	1.580262
Cl	0.046471	2.261335	-0.680124
Cl	2.320584	0.000000	-0.478765
Cl	0.009075	-2.220921	-0.693804
Cl	-2.310796	0.005495	-0.469030

[VOCl₄]²⁻ idealized structure

V	0.000000	0.000000	0.000000
O	0.000000	0.000000	1.580260
Cl	0.000000	2.281063	-0.581436
Cl	2.281063	0.000000	-0.581436
Cl	0.000000	-2.281063	-0.581436
Cl	-2.281063	0.000000	-0.581436

VOPc optimized structure

V	0.001035	1.963761	0.670096
O	0.013536	1.990117	2.223772
N	-2.363133	-0.405430	-0.002134
N	-0.003900	3.909584	-0.001001
N	-0.005040	-0.004750	0.070561
N	1.953075	1.951164	0.017611
N	-2.361792	4.308073	-0.091161
N	-1.961757	1.953021	0.051595
N	2.352410	4.305873	-0.133225
N	2.351007	-0.407660	-0.044669
C	-4.132573	1.255777	-0.117610
C	-0.702048	-2.176858	-0.082853
C	-1.111829	-0.790634	0.010793
C	-1.110256	4.692984	-0.092603
C	1.099815	-0.791716	-0.009031
C	-2.747125	3.057546	-0.047031
C	-4.132232	2.644712	-0.143690
C	-5.313816	0.536887	-0.208089
H	-5.309608	-0.529761	-0.190798
C	-2.747704	0.846170	-0.005495
C	1.101435	4.691974	-0.112146
C	2.737394	3.054987	-0.096047
C	2.736709	0.843588	-0.054852
C	-0.699652	6.074090	-0.241555
C	0.689516	6.073473	-0.253796
C	-1.417614	7.251880	-0.374597
H	-2.484383	7.247887	-0.368043
C	4.120011	2.640887	-0.219231
C	6.469019	1.242060	-0.439532
H	7.397208	0.720324	-0.525273
C	0.687062	-2.177554	-0.095308
C	4.119550	1.251921	-0.193417
C	-6.486340	1.248062	-0.318008
H	-7.416532	0.727207	-0.385479
C	5.299224	3.355203	-0.359416
H	5.295239	4.421756	-0.382028
C	5.298160	0.531980	-0.307038
H	5.293317	-0.534673	-0.290034
C	1.406010	7.250672	-0.399422
H	2.472728	7.245814	-0.411641
C	-6.486029	2.645764	-0.344287
H	-7.415994	3.164124	-0.431327
C	0.692479	8.420258	-0.524708
H	1.211699	9.347333	-0.634462
C	-0.709228	-4.532569	-0.258316
H	-1.230021	-5.463134	-0.320990
C	1.402914	-3.360049	-0.193105

H 2.469630 -3.356319 -0.205403
C -5.313248 3.360128 -0.261097
H -5.308709 4.426674 -0.283896
C -1.420778 -3.358580 -0.167825
H -2.487538 -3.353724 -0.161014
C 0.688625 -4.533289 -0.270846
H 1.207246 -5.464394 -0.342827
C -0.705402 8.420863 -0.512418
H -1.225650 9.348400 -0.613022
C 6.469518 2.639776 -0.465477
H 7.398104 3.157272 -0.570515

VO(acac)₂ optimized structure

V	-0.018195	0.010755	0.121557
O	0.005209	1.915790	-0.476822
O	1.893968	0.007354	-0.449106
O	-0.007813	-1.888934	-0.493419
O	-1.904506	0.018473	-0.533481
O	-0.050859	0.005127	1.670571
C	0.606481	4.139376	-0.871912
H	-0.092762	4.219741	-1.688151
H	1.463367	4.756905	-1.069173
H	0.107442	4.489596	0.016682
C	0.971280	2.694904	-0.683473
C	2.301788	2.295314	-0.757315
H	3.048367	3.031374	-0.939755
C	2.686579	0.962509	-0.656227
C	4.130237	0.580226	-0.813593
H	4.459353	0.090496	0.088534
H	4.760367	1.427495	-1.012434
H	4.217905	-0.131653	-1.618117
C	-0.579070	-4.103402	-0.971475
H	0.162389	-4.165780	-1.751292
H	-1.421828	-4.719309	-1.225976
H	-0.125722	-4.469511	-0.064815
C	-0.958099	-2.663603	-0.775153
C	-2.282303	-2.263159	-0.922857
H	-3.013820	-2.995976	-1.168345
C	-2.677762	-0.933951	-0.813415
C	-4.109898	-0.551458	-1.053659
H	-4.493439	-0.068545	-0.169622
H	-4.725779	-1.397302	-1.297662
H	-4.148744	0.166358	-1.856479

[VO(cat)₂]²⁻ optimized structure

V	1.895061	-0.000028	0.674427
O	1.774403	1.883734	0.024685
O	0.003568	0.040555	0.028336
O	1.895060	-0.000024	2.258811
C	0.566157	2.261253	-0.305902
C	-0.422647	1.231640	-0.303999
C	-1.723449	1.545441	-0.653205
H	-2.457947	0.765471	-0.650309
C	-2.074052	2.854767	-1.004666
H	-3.088336	3.078440	-1.271946
C	-1.122074	3.845718	-1.006398
H	-1.386487	4.849776	-1.275015
C	0.200769	3.547847	-0.656756
H	0.951247	4.312456	-0.656301
O	2.015715	-1.883795	0.024688
O	3.786551	-0.040619	0.028347
C	3.223961	-2.261315	-0.305899
C	4.212767	-1.231703	-0.303990
C	5.513567	-1.545502	-0.653200
H	6.248065	-0.765531	-0.650300
C	5.864170	-2.854827	-1.004665
H	6.878454	-3.078499	-1.271949
C	4.912192	-3.845776	-1.006403
H	5.176605	-4.849833	-1.275023
C	3.589349	-3.547908	-0.656758
H	2.838871	-4.312517	-0.656309

[VO(dmit)₂]²⁻ crystal structure

V	0.000000	0.000000	0.000000
S	2.262021	-0.056228	-0.759300
S	-0.014794	2.309492	-0.600700
S	4.231492	2.190239	-1.253500
S	2.233469	4.234192	-1.120200
S	5.044606	5.036901	-1.672400
O	0.000000	0.000000	1.593900
C	2.615920	1.635520	-0.925000
C	3.899295	3.886335	-1.378100
C	1.675843	2.604849	-0.851200
S	-2.262021	0.056228	-0.759300
S	0.014794	-2.309492	-0.600700
S	-4.231492	-2.190239	-1.253500
S	-2.233469	-4.234192	-1.120200
S	-5.044606	-5.036901	-1.672400
C	-2.615900	-1.635618	-0.925000
C	-3.899274	-3.886432	-1.378100
C	-1.675843	-2.604849	-0.851200

[V(bdt)₃]²⁻ crystal structure (H-optimized)

V	-0.107511	-0.026186	0.032267
S	-0.546563	-1.945633	-1.264193
S	-0.298407	2.004904	1.248317
S	-1.161104	1.260697	-1.678541
S	1.817730	0.034480	-1.340450
S	1.467973	-0.558606	1.733511
S	-1.792951	-0.933506	1.423530
C	-1.259884	2.922434	-1.139102
C	-2.322194	-2.458880	0.745734
C	-0.929790	3.238584	0.187999
C	-3.279656	-3.258608	1.377865
H	-3.693057	-2.932876	2.308629
C	-1.679043	3.949125	-1.992480
H	-1.918214	3.717964	-3.008513
C	3.217989	-0.312264	-0.355835
C	-1.052748	4.565194	0.638591
H	-0.793146	4.792873	1.650207
C	-3.701829	-4.449352	0.808372
H	-4.437618	-5.047751	1.305545
C	-1.777183	-2.886671	-0.470229
C	-2.209421	-4.103561	-1.034574
H	-1.787877	-4.420764	-1.964161
C	3.076040	-0.488422	1.028088
C	4.497174	-0.374282	-0.925996
H	4.596615	-0.256536	-1.983869
C	-1.801662	5.261358	-1.526687
H	-2.128110	6.030793	-2.196697
C	-1.486524	5.565226	-0.217117
H	-1.579162	6.570871	0.140439
C	5.610827	-0.575317	-0.138722
H	6.579998	-0.626496	-0.592984
C	4.222528	-0.641692	1.813037
H	4.113395	-0.751303	2.871191
C	-3.154721	-4.871902	-0.395429
H	-3.476984	-5.794347	-0.835516
C	5.483014	-0.694786	1.233204
H	6.348847	-0.826682	1.849461

[V(bds)₃]²⁻ crystal structure (H-optimized)

Se	-0.796476	-1.684988	1.522772
Se	1.756761	0.274502	1.746334
Se	1.584431	1.498826	-1.354509
V	0.006380	0.103548	-0.000151
C	3.177236	1.693532	-0.319571
C	-0.424266	-3.338051	0.659263
C	3.229502	1.205867	0.990272
C	-0.677815	-4.546355	1.331841
H	-1.002722	-4.522354	2.358112
C	4.400926	1.334215	1.735563
H	4.430788	0.942208	2.738545
C	4.304237	2.314421	-0.853775
H	4.272242	2.693058	-1.861872
C	-0.525425	-5.750243	0.667172
H	-0.728327	-6.675341	1.185324
C	5.464084	2.458579	-0.093638
H	6.325811	2.944630	-0.524889
C	5.519743	1.952871	1.195814
H	6.418720	2.054646	1.783705
Se	0.596286	-1.768326	-1.520292
C	0.034960	-3.365765	-0.654413
C	0.146624	-4.596337	-1.325138
H	0.471586	-4.611647	-2.351500
C	-0.144283	-5.773423	-0.658660
H	-0.056251	-6.716407	-1.176594
Se	-1.712523	0.473678	-1.747046
Se	-1.399123	1.674454	1.351856
C	-2.958696	2.050982	0.316483
C	-3.067275	1.570684	-0.992624
C	-4.215964	1.832875	-1.738113
H	-4.291952	1.444160	-2.739806
C	-4.006049	2.799178	0.849648
H	-3.931579	3.172963	1.857495
C	-5.141422	3.075708	0.089191
H	-5.943000	3.655311	0.521005
C	-5.255447	2.577913	-1.199400
H	-6.139252	2.777354	-1.785337

E. Representative ORCA Input Files

Representative ORCA input file for an optimization calculation

```
! UKS B3LYP OPT RIJCOSX ZORA ZORA-def2-TZVP def2/J TIGHTSCF GRID7 NOFINALGRID GRIDX9
NOFINALGRIDX
! LargePrint PrintBasis
%method
ScalHFX = 0.38
end
%scf
MaxIter 500
end
%pal nprocs 1
end
%maxcore 4500
%eprnmr
    gtensor 1
    ori -3
    printlevel 3
end
%tddft
nroots 15
maxdim 5
end
* xyzfile -2 2 /path/input.xyz
```

Representative ORCA input file for single point EPR & TDDFT calculation:

```
! UKS B3LYP SP RIJCOSX ZORA ZORA-def2-TZVP def2/J TIGHTSCF GRID7 NOFINALGRID GRIDX9
NOFINALGRIDX
! LargePrint PrintBasis
%method
ScalHFX = 0.38
end
%scf
MaxIter 500
end
%pal nprocs 1
end
%maxcore 4500
%eprnmr
    gtensor 1
    ori -3
    printlevel 3
end
%tddft
nroots 15
maxdim 5
end
* xyzfile -2 2 /path/input.xyz
```

Representative ORCA input file for frequency calculation:

```
! UKS B3LYP RIJCOSX FREQ def2-TZVP def2/J TIGHTSCF GRID7 NOFINALGRID GRIDX9 NO-
FINALGRIDX
! SlowConv
%method
ScalHFX = 0.38
Z_solver DIIS
Z_MaxIter 200
Z_shift 0.3
end
%scf
MaxIter 500
end
%pal nprocs 1
end
%maxcore 9000

*xyzfile -2 2 /path/input.xyz
```

References

- (1) Neese, F. The ORCA Program System. *Wiley Interdisciplinary Reviews: Computational Molecular Science* **2012**, 2 (1), 73–78. <https://doi.org/10.1002/wcms.81>.
- (2) Becke, A. D. A New Mixing of Hartree–Fock and Local Density-functional Theories. *J. Chem. Phys.* **1993**, 98 (2), 1372–1377. <https://doi.org/10.1063/1.464304>.
- (3) Lee, C.; Yang, W.; Parr, R. G. Development of the Colle-Salvetti Correlation-Energy Formula into a Functional of the Electron Density. *Phys. Rev. B* **1988**, 37 (2), 785–789. <https://doi.org/10.1103/PhysRevB.37.785>.
- (4) Vosko, S. H.; Wilk, L.; Nusair, M. Accurate Spin-Dependent Electron Liquid Correlation Energies for Local Spin Density Calculations: A Critical Analysis. *Can. J. Phys.* **1980**, 58 (8), 1200–1211. <https://doi.org/10.1139/p80-159>.
- (5) Stephens, P. J.; Devlin, F. J.; Chabalowski, C. F.; Frisch, M. J. Ab Initio Calculation of Vibrational Absorption and Circular Dichroism Spectra Using Density Functional Force Fields. *J. Phys. Chem.* **1994**, 98 (45), 11623–11627. <https://doi.org/10.1021/j100096a001>.
- (6) Szilagyi, R. K.; Metz, M.; Solomon, E. I. Spectroscopic Calibration of Modern Density Functional Methods Using $[\text{CuCl}_4]^{2-}$. *J. Phys. Chem. A* **2002**, 106 (12), 2994–3007. <https://doi.org/10.1021/jp014121c>.
- (7) Weigend, F.; Furche, F.; Ahlrichs, R. Gaussian Basis Sets of Quadruple Zeta Valence Quality for Atoms H–Kr. *J. Chem. Phys.* **2003**, 119 (24), 12753–12762. <https://doi.org/10.1063/1.1627293>.
- (8) Weigend, F. Accurate Coulomb-Fitting Basis Sets for H to Rn. *Phys. Chem. Chem. Phys.* **2006**, 8 (9), 1057–1065. <https://doi.org/10.1039/B515623H>.
- (9) Harlow, R. L.; Wells, W. J.; Watt, G. W.; Simonsen, S. H. Crystal Structures of the Green and Yellow Thermochromic Modifications of Bis(N-Methylphenethylammonium) Tetrachlorocuprate (II). Discrete Square-Planar and Flattened Tetrahedral Tetrachlorocuprate(2-)Anions. *Inorg. Chem.* **1974**, 13 (9), 2106–2111. <https://doi.org/10.1021/ic50139a012>.
- (10) McGinnety, J. A. Cesium Tetrachlorocuprate. Structure, Crystal Forces, and Charge Distribution. *J. Am. Chem. Soc.* **1972**, 94 (24), 8406–8413. <https://doi.org/10.1021/ja00779a020>.
- (11) Noll, A.; Rabe, S.; Müller, U. Die Oxochlorovanadate $\text{PPh}_4[\text{VOCl}_3\text{OH}]$, $\text{PPh}_4[\text{VOCl}_4]$, $(\text{PPh}_4)_2[\text{VOCl}_4]\cdot 2\text{CH}_3\text{CN}$ Und $(\text{PPh}_4)_2[\text{VOCl}_4]\cdot \text{CH}_3\text{CN}$ Mit Auffälligen Abweichungen von Der Quadratisch-Pyramidalen Anionenstruktur / The Oxochlorovanadates $\text{PPh}_4[\text{VOCl}_3\text{OH}]$, $\text{PPh}_4[\text{VOCl}_4]$, $(\text{PPh}_4)_2[\text{VOCl}_4]\cdot 2\text{CH}_3\text{CN}$ and $(\text{PPh}_4)_2[\text{VOCl}_4]\cdot \text{CH}_3\text{CN}$ with Remarkable Deviations from the Square-Pyramidal Anion Structure. *Zeitschrift für Naturforschung B* **1999**, 54 (5), 591–596. <https://doi.org/10.1515/znb-1999-0504>.
- (12) Konarev, D. V.; Kuzmin, A. V.; Faraonov, M. A.; Ishikawa, M.; Khasanov, S. S.; Nakano, Y.; Otsuka, A.; Yamochi, H.; Saito, G.; Lyubovskaya, R. N. Synthesis, Structures, and Properties of Crystalline Salts with Radical Anions of Metal-Containing and Metal-Free Phthalocyanines. *Chemistry – A European Journal* **2015**, 21 (3), 1014–1028. <https://doi.org/10.1002/chem.201404925>.
- (13) Wansapura, C. M.; Juyoung, C.; Simpson, J. L.; Szymanski, D.; Eaton, G. R.; Eaton, S. S.; Fox, S. From Planar Toward Tetrahedral Copper(II) Complexes: Structural and

- Electron Paramagnetic Resonance Studies of Substituent Steric Effects in an Extended Class of Pyrrolate-Imine Ligands. *Journal of Coordination Chemistry* **2003**, *56* (11), 975–993. <https://doi.org/10.1080/00958970310001607752>.
- (14) Atzori, M.; Benci, S.; Morra, E.; Tesi, L.; Chiesa, M.; Torre, R.; Sorace, L.; Sessoli, R. Structural Effects on the Spin Dynamics of Potential Molecular Qubits. *Inorg. Chem.* **2018**, *57* (2), 731–740. <https://doi.org/10.1021/acs.inorgchem.7b02616>.
- (15) Dodge, R. P.; Templeton, D. H.; Zalkin, A. Crystal Structure of Vanadyl Bisacetylacetone. Geometry of Vanadium in Fivefold Coordination. *J. Chem. Phys.* **1961**, *35* (1), 55–67. <https://doi.org/10.1063/1.1731933>.
- (16) Cassidy, P.; Hitchman, M. A. Molecular g Values of the Planar Tetrachlorocuprate(2-) Ion. *Inorganic Chemistry* **1977**, *16* (6), 1568–1570. <https://doi.org/10.1021/ic50172a067>.
- (17) Escalera-Moreno, L.; Suaud, N.; Gaita-Ariño, A.; Coronado, E. Determining Key Local Vibrations in the Relaxation of Molecular Spin Qubits and Single-Molecule Magnets. *J. Phys. Chem. Lett.* **2017**, *8* (7), 1695–1700. <https://doi.org/10.1021/acs.jpclett.7b00479>.